Advances in Geosciences Konstantinos Perakis & Athanasios Moysiadis, Editors
EARSeL, 2012

Ocean Remote Sensing in Support of Sea Level Anomalies and Mean Sea Surface Modelling

Georgios S. Vergos and Dimitrios A. Natsiopoulos
Aristotle University of Thessaloniki, Department of Geodesy and Surveying, Thessaloniki, Greece;
vergos@topo.auth.gr, anatsiopoulos@hotmail.com

Abstract. The exploitation of altimetric data sets from past and current satellite missions is fundamental to both oceanographic and geodetic applications. For oceanographic studies it allows the determination of sea level anomalies, as deviations from a static mean sea level, while it is also fundamental for marine geoid and gravity determination. With the advent of the recent gravity-field dedicated missions of GRACE and GOCE, an abundance of gravity data for the oceans became available as well. A crucial point to studying the variations of the sea surface is proper combination of heterogeneous data, with a statistically rigorous method. The optimal operator for such purposes, used in physical geodesy, is least squares collocation, which needs the input data and error variance-covariance matrices to be known. In this work, altimetric data sets from the satellite remote sensing missions of Jason-1 and ENVISAT have been used to study variation in the sea level and determine of Mean Sea Surface (MSS) models in the Mediterranean Sea. The raw data used are Sea Level Anomaly (SLA) values and their total inverse barometer corrections from the respective altimetric missions acquired by the on-board altimeters. Along-track records of the SLA have been used both to derive linear trends of the SLA variation in the area under study and come to some conclusions on the Mediterranean variability at scales as short as ten days. Empirical covariance functions and the statistical analysis of the SLA along-track repeated satellite records are presented and used to study the variations of the sea level between 2005 and 2010. Moreover, the estimated SLA variations are correlated with climatic indexes like SIO, NAO and MOI in order to conclude on the contribution of atmospheric forcing to the steric part of sea level fluctuations. Finally, the available SLAs are used along with the estimated covariance function to determine single and multi-satellite models of the mean sea surface through least squares collocation, which are then validated against the DTU2010 MSS model.

Keywords. Satellite altimetry, mean sea surface, sea level anomalies, covariance functions.

1. Introduction

Fluctuations in the level of the sea pose an issue of emerging importance, since latest scientific research shows a clear trend in the rise of the sea level. This of utmost importance especially for Europe, since one of the most over-crowded coastlines in the world lays across the Mediterranean Sea. The current population of the Mediterranean Basin countries is around 380 million with 146 million (~39%) living along the coast itself. According to demographic projections worked out by the Mediterranean Action Plan [1], the Mediterranean Basin's resident population could reach as high as 555 million within 30 years. By 2025, the Mediterranean could be hosting up to 350 million seasonal tourists a year as well. In a global scale, 44% of the world's population lives within 150 km of the coast. In 2001 over half the world's population lived within 200 km of a coastline.

The rate of population growth in coastal areas is accelerating and increasing tourism adds pressure on the environment. The more people crowd into coastal areas, the more pressure they impose both on land and sea and in particular in natural ecosystems and protected areas. Natural landscapes and habitats are altered, overwhelmed and destroyed to accommodate them. Lagoons and coastal waters are 'reclaimed', wetlands are drained and covered with rubbish, floodplains

around estuaries are built over and reduced, while mangroves and other forests are cut down. Ecosystems are damaged, frequently lost forever. Fresh water, soils and beach sands are often overexploited, at great economic and ecological cost [2]. It goes without saying that a rise in the level of the sea will influence a large number of people. Additionally, it will have a significant impact on all environmental aspects of life as well as on the natural environment itself and the delicate balance on the ecosystems that resides in area close to the coastline. Coastal areas host a rich set of natural and economic resources and include some of the most developed and rapidly growing population centers both globally and in particular in the Mediterranean and Black Sea. Changing sea levels can inundate low-lying wetlands and dry lands, erode beaches, change rates of sedimentation, and increase the salinity of marshes, estuaries, and aquifers [3], [4]. Documented consequences of sea level rise include loss of buffering against storms and floods, changes in bird populations and land cover, property losses, and infrastructure damage [5], [3], [4].

During the last century, the global average sea level rose by 17 cm while projections for the future direct towards a continued rise in the sea level. Therefore monitoring the sea level and its fluctuations with time is mandatory within every environmental monitoring protocol and system. As it has been shown by [6] an ~18.5 cm of sea level rise can be found from the available global tide-gauge data for the period between 1900 and 2000. For comparison, the recent annually averaged satellite altimetry data from TOPEX/Poseidon, ENVISAT and Jason 1/2 show a somewhat higher rate of increase than tide gauge (TG) data. Many factors affect the temporal and long-term variations of the sea level, including, but not limited to, changes in sea temperature, salinity, and total water volume and mass [7]. Sea level rises with warming sea temperatures and falls with cooling, showing a direct correlation with El Niño/La Niña Southern Oscillation (ENSO) events. Therefore, the changes in the global average sea level indicate the environmental physical and climatic stability at a global scale [7]. In conclusion, a clear trend in sea level rise is evident and much of that has been attributed to global warming, while a lesser part is attributed to thermal expansion of Earth itself. Based on the aforementioned facts, it is vital to monitor the variations and trends in sea level since it can be identified as one of the key components in environmental monitoring system.

Monitoring of the sea level has been traditionally carried out with tide-gauge stations located in coastal areas around the globe. This situation arrived at a landmark during the last 30 years, with the early missions of GEOS-3 and SeaSat in the mid ‘70s to the recent ones of Jason-2 and ENVISAT, when altimeters onboard satellites offered an unprecedented database of instantaneous measurements of the sea surface. The basic altimetric measurement refers to the satellite height above the non-static sea surface, determined as the two-way travel time needed for the radar pulse emitted from the satellite to reach the sea surface and received by the instrument’s receiver (Figure 1, [8]). The difference between that height and the altitude of the satellite above a reference ellipsoid leads to the determination of the instantaneous sea surface height (SSH), which successfully represents the geometric height of the non-static sea surface. This abundance of measurements for the Earth’s oceans leads to an improved knowledge of the monitoring of sea level variations over large time and spatial scales. Repeated satellite altimetry data span nowadays over a period of about 35 years, if one considers the exact repeat mission (ERM) of GEOSAT as a landmark and the latest missions of Jason-2 and ENVISAT. This record of measurements about the variations and mean level of the Earth’s oceans, manage to provide reliable monitoring tools for time periods as short as ten days, useful for sea level anomaly determination, and long enough in order to provide a more-or-less reliable estimate of trends in mean sea level (MSL) rise [9].

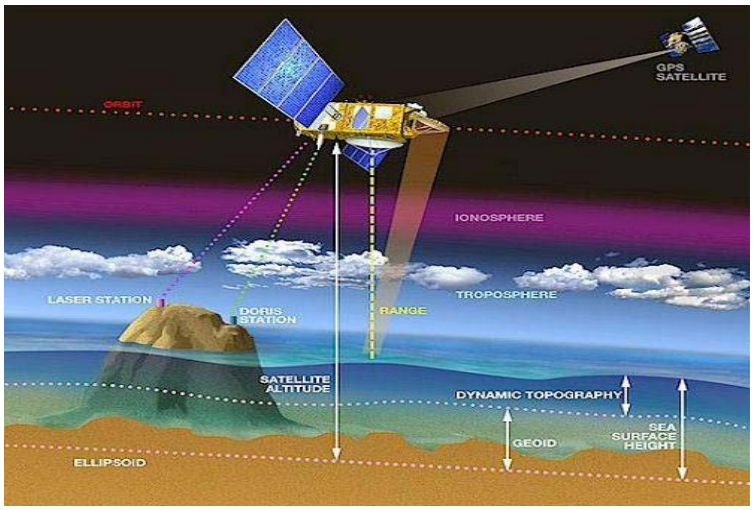

Figure 1: Principle of satellite altimetry (credit (8)).

As far as the determination of mean sea surface (MSS) models from satellite altimetry data is concerned, many studies have been conducted in the past, presenting either global models [10], [11], [12], [13], or regional ones [14], [15], [16], [17], [18], [19], [20], [21], the latter mainly in the form of altimetric marine geoid models. Satellite altimetry observations have provided for the first time homogeneous and almost-global coverage, high-resolution and precision observations for the instantaneous sea surface compared to the traditional shipboard data. Therefore, they offer a powerful tool in order to monitor and model processes that take place on the surface of the oceans, such as sea level variations, rise/fall, ocean circulation, etc. [22], [23], [24] and in their interior through inverse modelling, e.g., currents, temperature/salinity/pressure variations, etc.. A very good review on the applications of satellite altimetry to geodesy and sea level changes is given by [25] and [26] respectively.

Within the aforementioned frame, the aim of the present study is to first analyse available Jason-1 and ENVISAT observations of sea level anomalies (SLAs) in the wider area of the Mediterranean Sea. Even though the Mediterranean is a semi-closed sea basin, with limited span especially in the north-south direction, the availability of repeated altimetric tracks allows monitoring of variations with time of the sea level at spans as short as the repeat period of the available satellite data. In that way, seasonal and temporal variations of the sea level can be studied, while conclusions on the existence of long-term trends can be derived as well. Given that the available data in the present study came from the Jason-1 (Phase A) and ENVISAT missions, the variation of SLA within the repeat period of the former (10 to 35 day periods) has been investigated for selected cycle. The second goal is to develop MSS models based on single- and multi-mission satellite altimetry data using least squares collocation (LSC). The latter is well-established, especially in geodetic research as the leading estimation principle within a least squares prediction scheme. It is based on the determination of some output stochastic signal(s) according to the availability of input data which are inter-related with the outputs with some covariance function in the sense that all variance-covariance matrices for the adjustment are derived from one basic covariance function [27], [28], [29]. In LSC, and in order to construct the necessary covariance and cross-covariance matrices, it is necessary to fit some analytical model to empirical values, so that within the scheme of the present study, the Tscherning and Rapp model was fitted to the empirical SLA covariance functions derived from the available data [30]. Given that the selection of the correlation length is vital for the construction of the necessary covariance and cross-covariance matrices, a study of the varying behaviour of the empirical covariance models was performed in relation to the cross- and along-track spacing of the available satellite data. From that latter step, conclusions on the evidence of the cyclo-stationarity of the SLA can be deduced and correlated with

climate change indices over the oceans, such as the Southern Oscillation Index (SOI) corresponding to the ocean response to El Niño/La Niña-Southern Oscillation (ENSO) events, the North Atlantic Oscillation index (NAO) and the Mediterranean Oscillation Index (MOI) .

2. Area under study, available data and pre-processing

The area under study spans the entire Mediterranean Sea bounded between $30^o \leq \varphi \leq 50^o$ and $-10^o \leq \lambda \leq 40^o$. As already mentioned in the previous section, the data employed in the present work are those of the Jason-1 and ENVISAT missions. For Jason-1, data during the period from 15/1/2002 (cycle 1) to 07/12/2008 (cycle 255) have been used resulting in a total number of 670703 observations (Figure 2, Jason -1 data distribution). Each Jason-1 cycle consists of 254 passes with almost 20% of those having available observations in the Mediterranean Sea within the satellite's period of 10 days. As far as ENVISAT is concerned, 678258 point values (Figure 3, ENVISAT data distribution) have been collected, within the period 24/09/2002 and 25/03/2009 (cycle 1 to cycle 77). The mesh of values is much denser than Jason-1 and is composed by about 1003 passes. Its cross track spacing is 75 km at the equator compared to 300 km for Jason-1. The data used have been downloaded from the Radar Altimeter Database System (RADS, 32) operated by the Delft Institute for Earth-Oriented Space research (DEOS) [31]. RADS presents a collection of almost all past and current satellite altimetry and is DEOS' effort in establishing a harmonized, validated and cross-calibrated sea level data base from satellite altimeter data. The selection of RADS to collect the Jason-1 and ENVISAT observations was based on the facts that a) harmonized geophysical corrections for all data were needed compared to using various geophysical models, e.g. from AVISO for Jason-1 [32], b) the SLAs datum in terms of the reference ellipsoid needed to be unified in order to avoid datum inconsistencies that would result in biases when computing multi-satellite solutions [33], [17], c) the SLAs from both satellites were needed in a unified and commonly crossover adjusted orbit reference frame (see below on the selection of the orbit reference frame of the data used) and d) easiness and one-stop place data collection for both satellites.

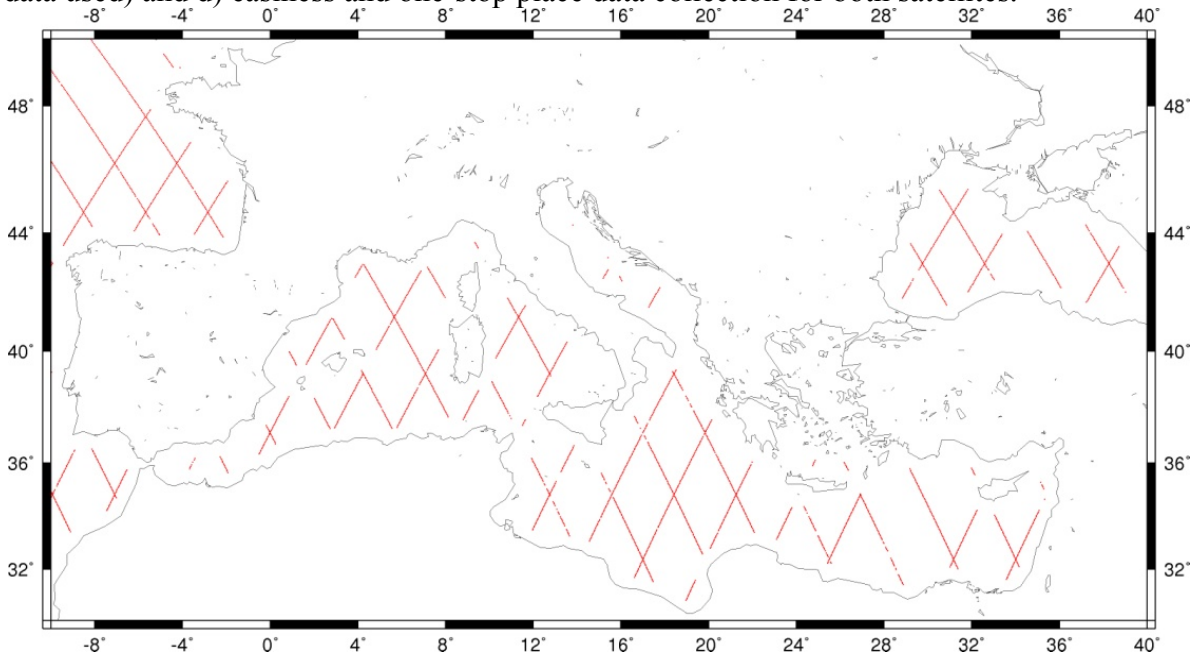

Figure 2: Jason-1 data distribution.

The altimetric data were available in the form of SLAs referenced to a *"mean-sea*-surface*"* that depends on user selection within the RADS system. Therefore, it was decided to refer the data to the EGM2008 geoid [34]*, keeping in mind that a zero-tide (ZT) geoid model is adopted to be in-line*

with the tide-conventions used in altimetric data processing. As far as the selection of the geophysical corrections and models used, those were a) ECMWF for the dry tropospheric correction, b) MWR(NN) for the wet tropospheric correction, c) the smoothed dual-frequency model for the ionospheric correction, d) tidal effects due to Solid Earth, Ocean, Load and Pole from the Solid Earth tide, GOT4.7 ocean tide, GOT4.7 load tide and pole tide models respectively, and e) the CLS Sea State Bias (SSB) model for the SSB effect. [35] and the references herein should be advised for more details on the models used. All geophysical corrections mentioned previously have been applied to the Jason-1 and ENVISAT raw observations, in order to construct corrected geophysical data records, i.e., corrected SLAs referenced to the EGM2008 ZT geoid.

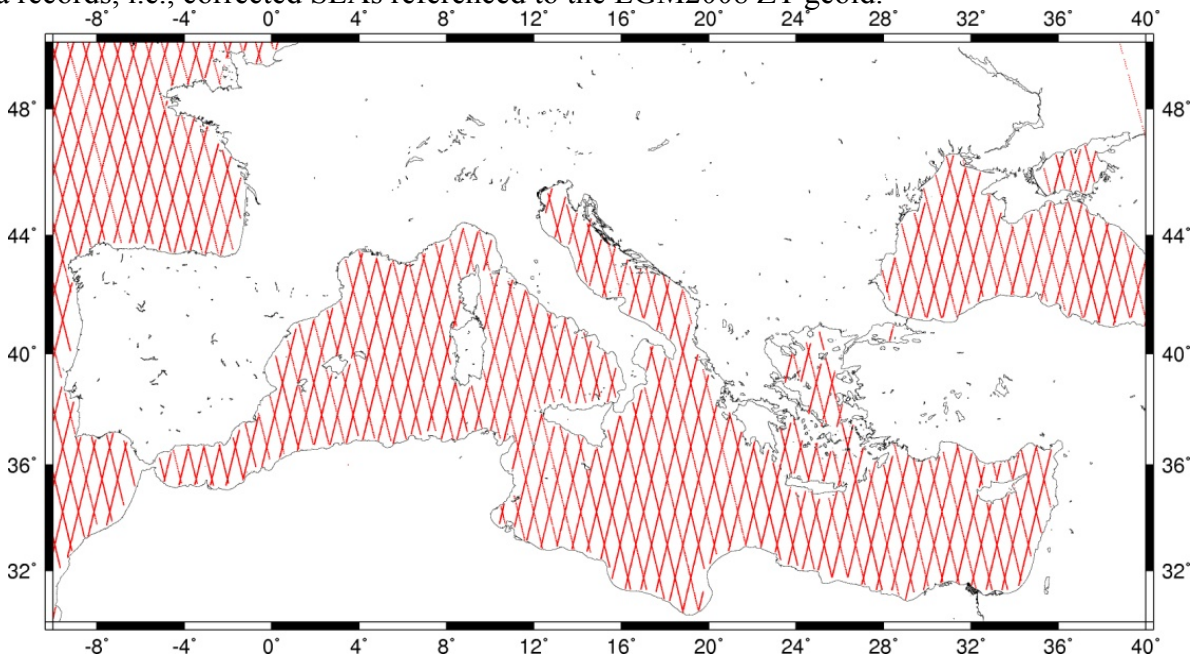

Figure 3: ENVISAT data distribution.

As far as the Inverse Barometer (IB) correction is concerned, this has been applied at a second stage to the available SLA data, during which, both the global and local IB corrections were used. Tables 1 and 2 below summarize the statistics of the corrected SLA values for the geophysical effects, before and after the total inverse barometer corrections. From these Tables, it is obvious that the total inverse barometer correction has little effect to the "global" SLA statistics, i.e., the range of the values and their mean and standard deviation (std). The maximum and minimum values shown are clearly due to blunders in the available SLA data and they are located in all cases close to the coastline. Before proceeding any further to the utilization of the SLA data for MSL or sea level variations studies, a 3σ test has been applied in order to remove blunders. It should be noted that in order to apply such a blunder detection and removal test, the data are regarded as bias free, which for the case of the JASON-1 and ENVISAT observations holds since the mean value of the former is at the 9 mm level and that of the latter close to 3 cm. Such small mean values can be safely regarded as close to zero, so that the data can be treated as bias free. The meaning of the 3σ test is that all SLA values that exhibit a value of 3σ in an absolute sense, are regarded as blunders and are removed from the database. Table 3 below summarizes the statistics of the JASON-1 and ENVISAT SLAs after the 3σ removal test (see the top row of Tables 1 and 2 for comparison). As far as JASON-1 data are concerned, only 6344 (less than 1%) observations were removed as blunders, while the reduction of the data range is significant from ~2.6 m to 0.88 m only. From the ENVISAT SLAs, a total number of 8502 observations are removed (~1.2), again reducing the range of the data significantly, from ~3.9 m to 0.86 m only. These latter blunder-free observations will

form the basis for the investigation of SLA variations and the determination of MSS models in the area under study.

Table 1. Statistics of Jason-1 data before and after the total IB correction. Unit: [m].

	nr. values	min	max	mean	std
SLA	653789	-1.817	0.880	0.009	±0.150
SLA+total inv. barom. cor	653789	-1.914	1.083	-0.044	±0.189

Table 2. Statistics of ENVISAT data before and after the total IB correction. Unit: [m].

	nr. values	min	max	mean	std
SLA	678255	-2.781	1.179	0.028	±0.143
SLA+total inv. barom. cor	678255	-2.748	1.315	0.078	±0.163

Table 3. Statistics of Jason-1 and ENVISAT SLAs after the 3σ. Unit: [m].

	nr. values	min	max	mean	std
Jason-1 SLAs	647445	-0.447	0.447	0.010	±0.141
ENVISAT SLAs	669753	-0.433	0.433	0.022	±0.133

3. Sea level anomaly variations in the Mediterranean Sea

The first part of this work refers to the identification of sea level variations within the satellite repeat period, i.e., for periods as short as 10 days (actually 9.9 days) for Jason-1 and 35 days for ENVISAT. In order to investigate such variations, a single pass was selected from each satellite based on the following criteria: a) the pass shall be long and span the entire basin in the north-south or south-north direction (ascending or descending pass respectively), b) there shall be no or little land intrusion from isles or islands in the pass SLA records, c) the data record shall be as consistent as possible throughout the satellite data record for the period of study, i.e., missing records and/or voids should be kept to a minimum. Based on these criteria, it was decided that pass 196 would be studied for Jason-1and pass 399 for ENVISAT. Jason-1pass 196 is an ascending pass leaving Africa in the coastal areas of Libya, continuing north to the Ionian Sea and ending to the south-east part of Italy. On the other hand, ENVISAT pass 399 is a descending one crossing the entire eastern Aegean Sea, starting in the north off the coast of Thasos, crossing Lemnos, then east Cyclades, and finally after crossing the strait between Crete and Karpathos enters the Libyan Sea and ends over the coasts of Egypt. Figure 4 below depict the two passes investigated, where the red colour denotes Jason-1's pass 196 and the blue color ENVISAT's pass 399. The analysis presented herein refers to the aforementioned tracks for each satellite, therefore along-track SLA variations are studied rather than basin-wide.

3.1. Sea level anomaly variations from Jason-1

The study period for the Jason-1 SLA data is between cycle 1 (15/01/2002) and cycle 255 (07/12/2008). Table 4 below summarizes the statistics of the annual Jason-1 SLAs after the application of all geophysical corrections including that of the global and local IB ones. From that Table it is evident that the available annual Jason-1 SLAs do not present a significant variation, since from 2002 until 2008 the std varies by ~2 cm, while some noticing variations can be viewed

in the range of the observations only. Therefore, it becomes apparent that a more detailed outlook per-cycle and track is needed in order to detect SLA variations.

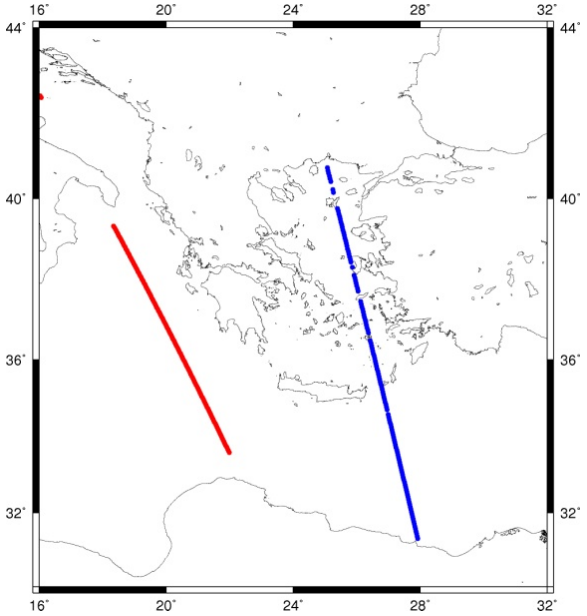

Figure 4: Jason-1 pass 196 (red) and Envisat pass 399 (blue) used for SLA variation monitoring.

Table 4. Statistics of annual Jason-1 SLAs.

YEAR	cycles	min	max	mean	std
2002	1-36	-0.472	0.771	0.018	±0.142
2003	37-73	-1.239	0.695	-0.007	±0.148
2004	74-110	-0.690	0.793	0.009	±0.164
2005	111-146	-0.631	0.690	0.011	±0.156
2006	147-183	-0.543	0.800	0.012	±0.152
2007	184-220	-1.817	0.880	-0.005	±0.136
2008	221-255	-0.842	0.791	0.021	±0.144

Starting from cycle 1 for pass 196, the Figures and Tables given below present a) the available SLAs for the same pass and three consecutive cycles, so that a full month is covered (e.g., cycle 1 is analysed together with cycles 2 and 3 so that a total of ~30 days is studied), and b) the SLA residuals between the studied cycles, i.e., the differences between the available SLAs for the three consecutive cycles studied. Figures 5 and 6 present the available SLAs for pass 196 and cycles 1, 2 and 3 as well as their differences. In all Figures the horizontal axis refers to geographic latitude and the vertical one to SLAs or SLA differences in m.

From Figure 5 (top), it becomes evident that a good correlation between the SLA data between cycles 1 and 2 exists, while cycle 3 deviates significantly from the other two. This deviation can be viewed as a constant bias between the three cycles of the order of 10 cm. It should be noted that the SLA data are already corrected for the IB effect, so this deviation cannot be attributed to the sea surface response to the change of the air pressure. From Figure 6, where the SLA differences between cycles 1, 2 and 3 are plotted a linear trend, i.e., change in the sea level, between -1.2 cm and 3.1 cm per 9.9 days can be seen. The latter trend of 3.1 cm/10 days is found between cycles 2 and 3, signaling that a significant variation in the sea level occurred between these days. It should be noted that these cycles refer to January 2002, so the same analysis has been performed for

available SLAs in January 2006 (cycles 147, 148 and 149) and January 2008 (cycles 221, 222 and 223).

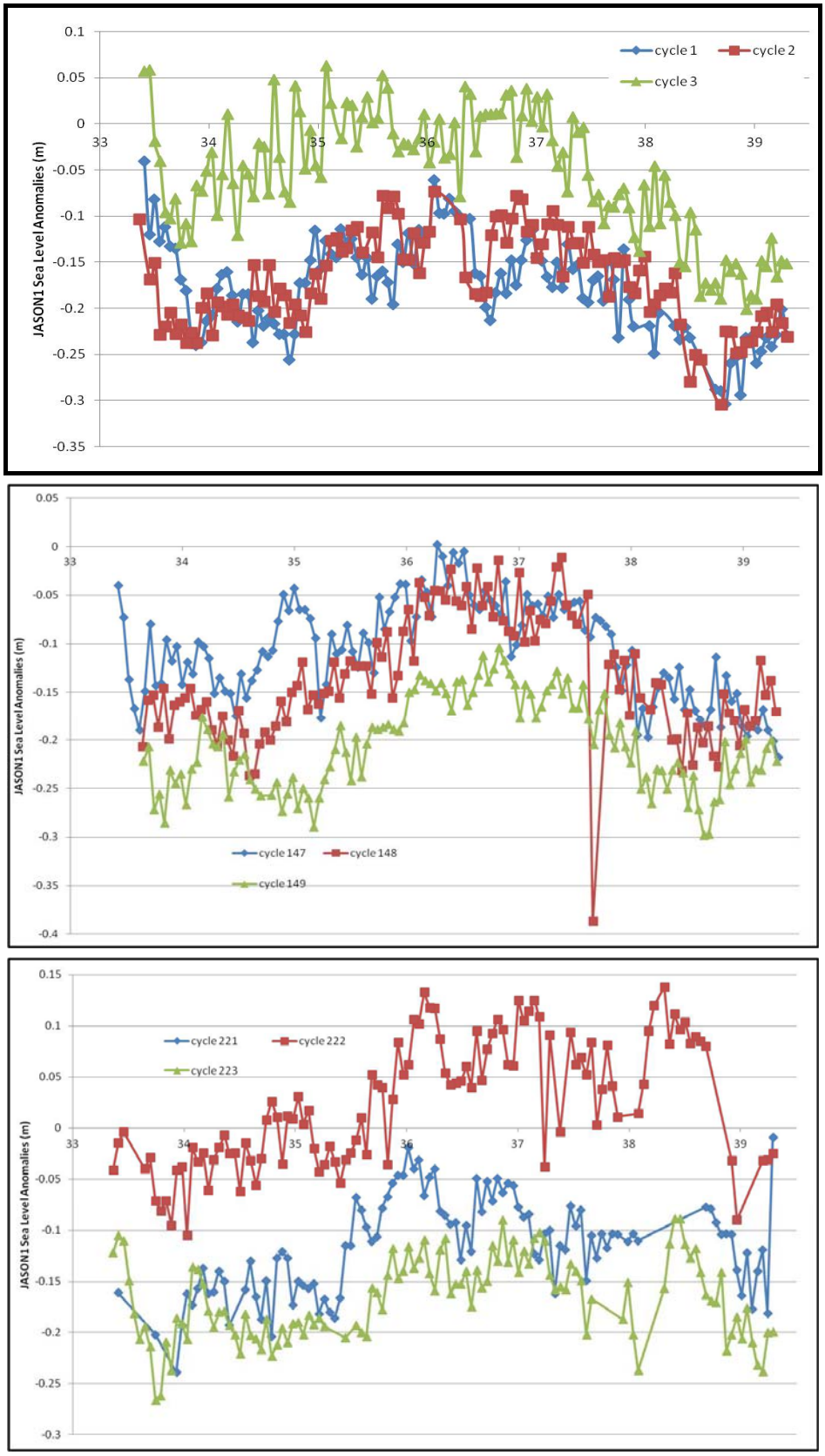

Figure 5: Jason-1 pass 196 SLAs for cycles 1, 2 and 3 (top), cycles 147, 148 and 149 (middle) and cycles 221, 222 and 223 (bottom).

From Figure 5 (bottom), the same good correlation between cycles 147 and 148 (corresponding to cycles 1 and 2) can be found, while again cycle 149 (corresponding to cycle 3) presents a bias of the order of 15 cm. From Figure 7, a linear trend of -2.1 cm/20 days and -2 cm/10 days is found between cycles 147 and 149 and 147 and 148 respectively. This situation reverses in 2008 when analyzing cycles 221, 222 and 223 (corresponding to cycles 1, 2 and 3 respectively), since now the ones that are 30 days apart present a better correlation than the 10 day ones (Figure 5, bottom). The bias between the SLA data is now at the 10 cm level, while the trend ranges between 2.7 cm/10 days and 1.1 cm/20 days (Figure 8).

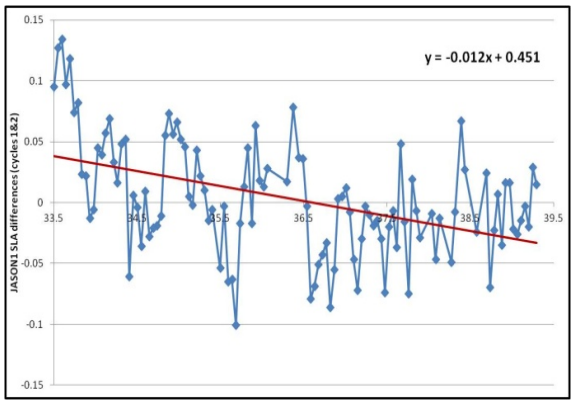

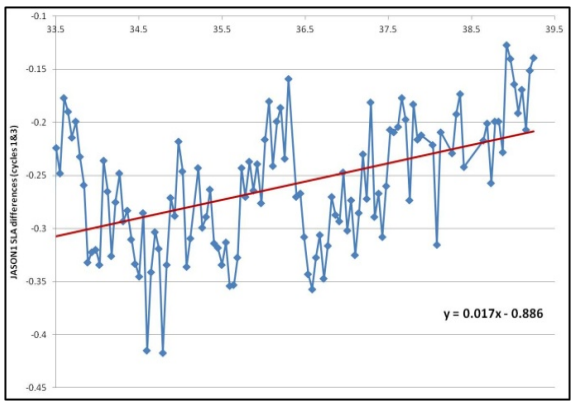

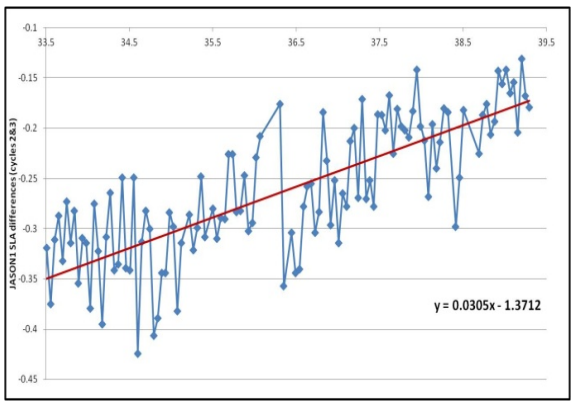

Figure 6: Jason-1 SLA differences and linear trend for pass 196 between cycles 1 and 2 (top), 1 and 3 (middle), 2 and 3 (bottom).

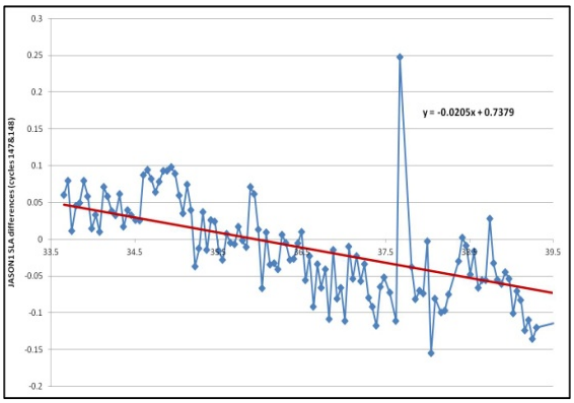

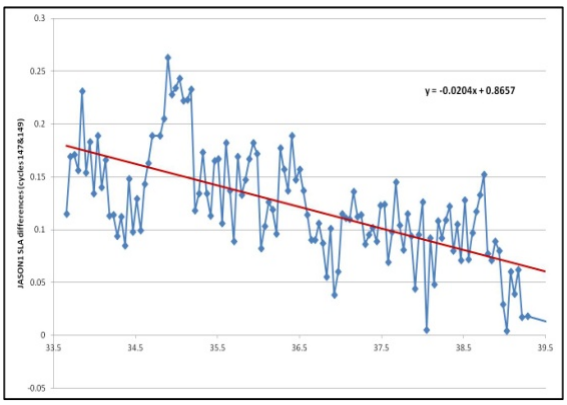

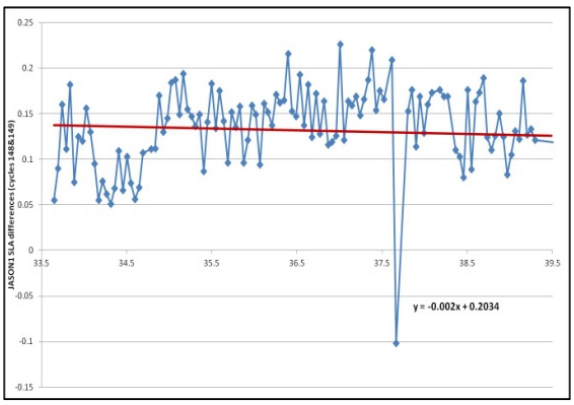

Figure 7: Jason-1 SLA differences and linear trend for pass 196 between cycles 147 and 148 (top), 147 and 149 (middle), 148 and 149 (bottom).

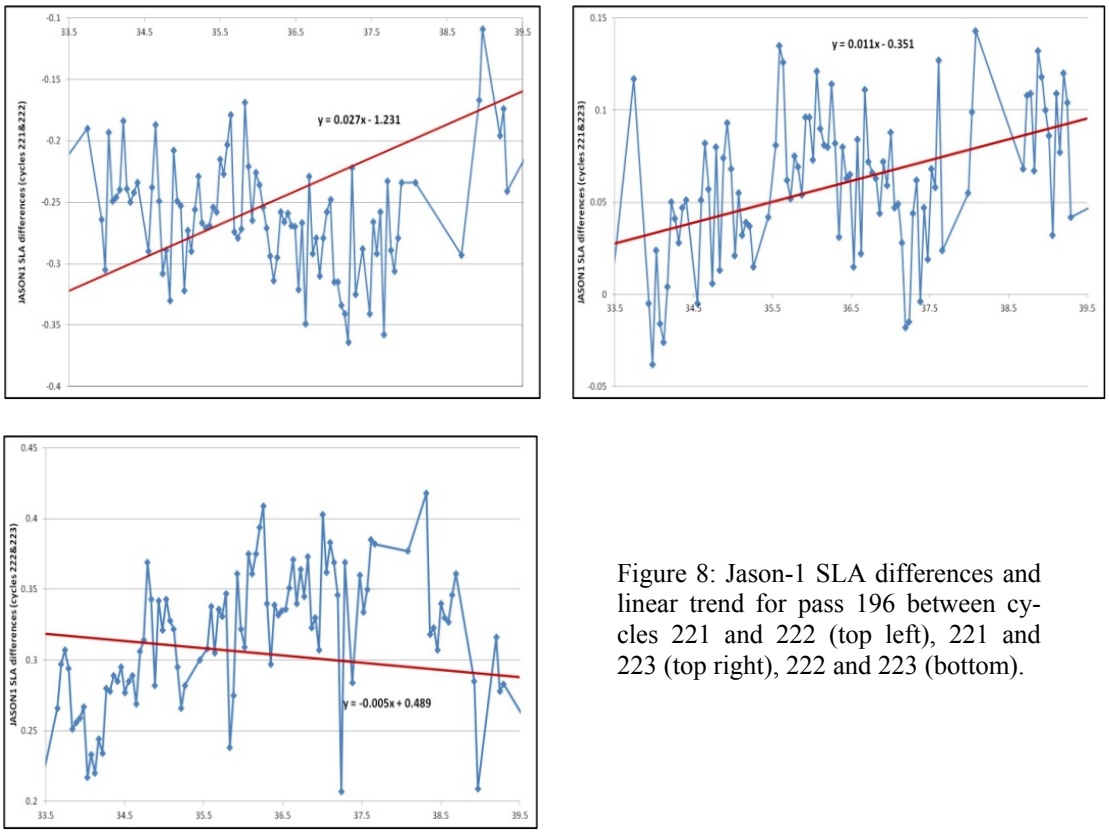

Figure 8: Jason-1 SLA differences and linear trend for pass 196 between cycles 221 and 222 (top left), 221 and 223 (top right), 222 and 223 (bottom).

3.2. Sea level anomaly variations from ENVISAT

The study period for the ENVISAT SLA data is between cycle 13 (13/03/2003) and cycle 75 (24/01/2009). Table 5 below summarizes the statistics of the annual ENVISAT SLAs after the application of all geophysical corrections including that of the global and local IB ones. From that Table a variation of the order of ~2 cm can be seen in the std, which is in agreement with the findings from JASON1. The large discrepancies in the minimum value of year 2007 can be attributed to same blunders still existing in the SLA records.

Table 5. Statistics of annual Jason-1 SLAs. Unit: [m].

YEAR	period	cycles	min	max	mean	std
2003	13-1-03 to 2-2-04	13-23	-0.773	0.911	0.013	±0.138
2004	2-2-04 to 17-1-05	24-33	-0.802	1.061	0.026	±0.154
2005	17-1-05 to 2-1-06	34-43	-1.142	1.179	0.029	±0.153
2006	2-1-06 to 22-1-07	44-54	-1.391	0.893	0.026	±0.149
2007	22-1-07 to 7-1-08	55-64	-2.781	0.792	0.028	±0.130
2008	7-1-08 to 24-1-09	65-75	-0.727	0.798	0.030	±0.134

Starting from cycle 23 for pass 399, the Figures and Tables given below present a) the available SLAs for the same pass and three consecutive cycles, so that more than three months are covered (e.g., cycle 23 is analysed together with cycles 24 and 25 so that a total of ~105 days is studied), and b) the SLA residuals between the studied cycles, i.e., the differences between the available

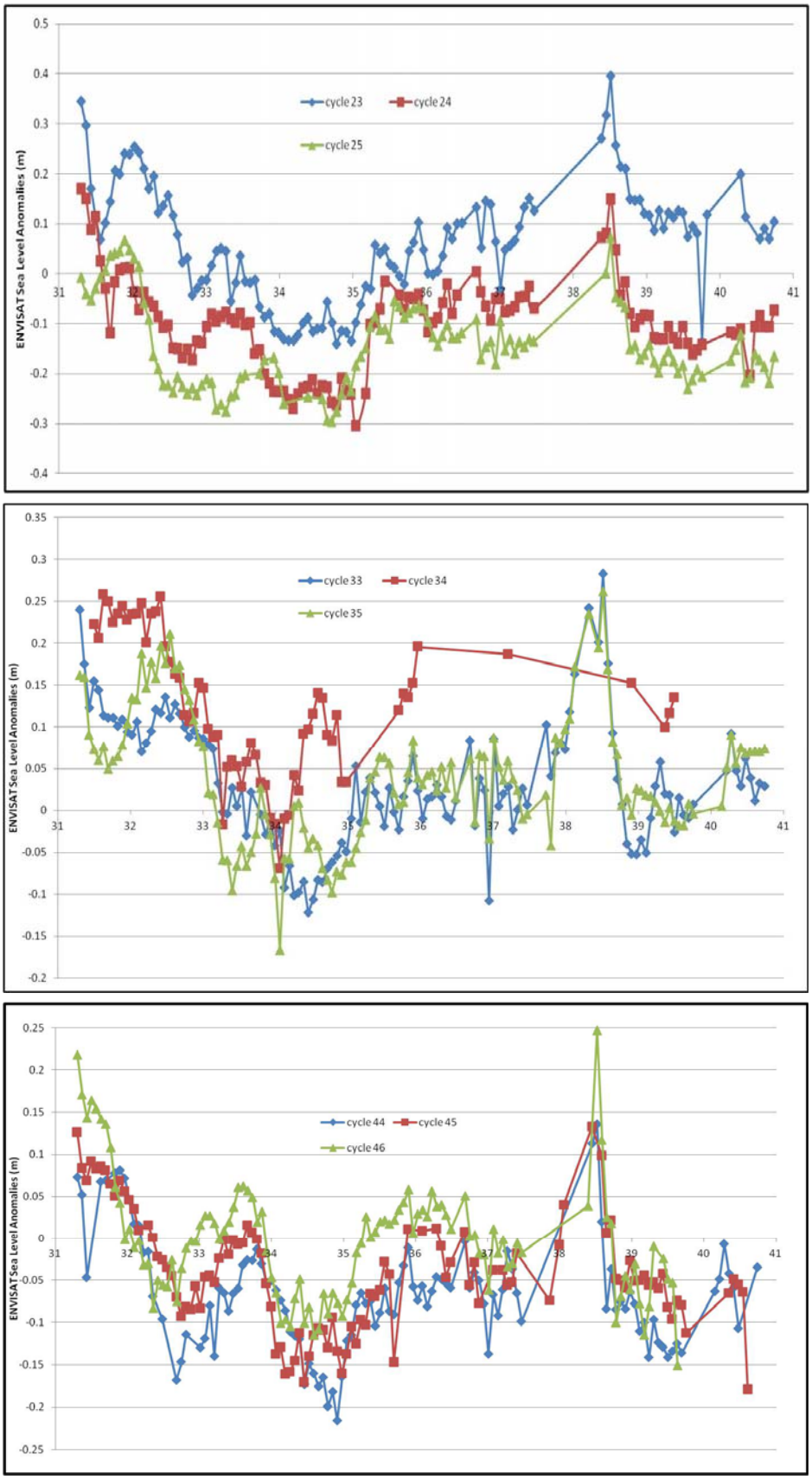

Figure 9. ENVISAT pass 399 SLAs for cycles 23, 24 and 25 (top), cycles 33, 34 and 35 (middle) and cycles 44, 45 and 46.

SLAs for the three consecutive cycles studied. It should be pointed out that the cycles analysed herein cover always the first three months of each year, while year 2006 SLAs, already analysed with Jason-1 (cycles 147-149), are studies with ENVISAT as well (cycles 44-46). Note that the SLA variations presented by JASON1 are not directly comparable with those of ENVISAT, since they refer to different time scales, the former presenting a variation between 10 and 30 days and the latter a variation between 35 and 105 days.

Figures 9 and 10 present the available SLAs for pass 399 and cycles 23, 24 and 25 as well as their differences. In all Figures the horizontal axis refers to geographic latitude and the vertical one to SLAs or SLA differences in m. From Figure 9 (top) a mean separation between the repeated ENVISAT cycles is evidenced, of the order of ~10 cm, while if this bias is neglected, the SLA records follow the same periodic pattern of decreased and increased sea level with increasing latitude. Therefore, it is expected that a trend within these three cycles would not be evident. This is confirmed from Figure 10, where the SLA differences between cycles 23, 24 and 25 are presented, since the estimated trends are between +4 mm/35-days and -2 mm/35-days.

From Figure 9 (middle) where the respective SLAs for cycles 33, 34 and 35 are plotted, it is interesting to notice that cycle 34 misses a significant number of records compared to the other, so that no data are available north of $\varphi=39.5^o$. Moreover, cycle 34 follows closely the other two cycles analyzed until $\varphi=34.3^o$ (approximately at the south-east corner of Crete), and as the satellite moves to northern latitudes it deviates significantly with a bias of the order of ~15-20 cm. This is a good indication that the available SLA records from that cycle contains blunders, since when investigating the mean wind-speed for each cycle it was found that they do not deviate significantly (the wind speed ranges between 6.6 m/s, 10.7 m/s and 7.2 m/s for cycles 33, 34 and 35 respectively). Therefore, wind-drives SLA variations that were not treated by the applied IB correction cannot be blamed for the deviations found. When investigating the differences between the three cycles (Figure 11) it is found that a positive trend of +6 mm/35-days exists between cycles 34 and 35, while a negative trend of –5 mm/35-days exists between cycles 33 and 34. As a consequence, no trend is found in the 3-month period covered by cycles 33 and 35.

Figure 9 (bottom), presents the SLA records for cycles 44, 45 and 46 covering the first three months of 2006, where an interesting agreement is found between the consecutive records of the satellite. This signals that almost no bias exists between the SLA records, since this is at the 5 cm level at most. Once again, one cycle misses a significant number of records, that is cycle 46, since no SLA data are available north of $\varphi=39.6^o$. Nevertheless, the same problems as with cycle 34 are not evidenced for the rest of the cycle records, since they do not present any extreme, blunder-like, variations compared to cycles 44 and 45. From that analysis of the differences between the SLAs (Figure 12), a zero trend is found between cycles 44 and 45, while the sea rises by +2 mm/35-days between cycles 45 and 46, so that the same trend holds between cycles 44 and 46 as well.

It is quite interesting to investigate the possible correlations between ENVISAT and JASON1 SLAs that belong to approximately the same time period and examine is the same level of SLA trend is derived. As it was presented in Figure 4, the ENVISAT and JASON1 tracks do not cover the same geographical area, while the ocean circulation pattern in the Adriatic Sea and the Aegean Sea are quite different. Nevertheless, it would be interesting to investigate if this collocated analysis can give some meaningful results.

Figure 13 presents the SLAs from the respective satellite records, where a very good agreement can be found between JASON1 and ENVISAT. It should be noted that the SLA records plotted in that Figure refer to the original location of each satellite, so no interpolation to a mean latitude has been performed in order to maintain the inherent accuracy of the data. This good agreement can be also viewed in the determined correlation coefficient between the SLA records, which is at the 50.2% level. If one considers that the available records refer to different locations, which are ~350

km apart, it becomes evident that the combined analysis of multi-mission altimetry data at collocated epochs can lead to an improved analysis of the variations of the sea level. In terms of the determined SLA trends, a very good agreement was once again found, since JASON1 records give a trend of +0.9 mm compared to 0.3 mm for ENVISAT. Given the error budget of satellite altimetry, it is evident that both satellites determine a zero level trend for the period investigated, confirming their good agreement.

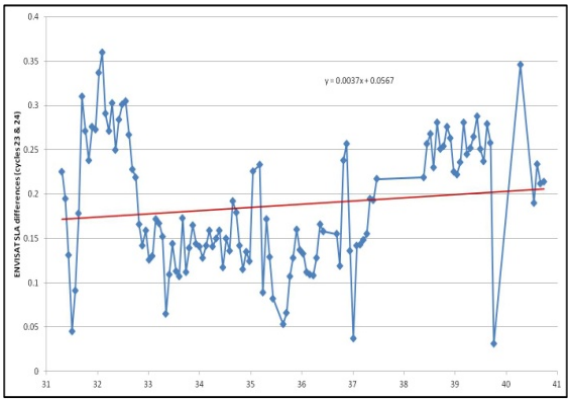

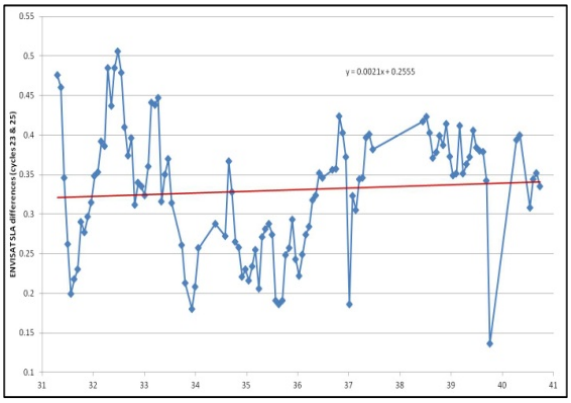

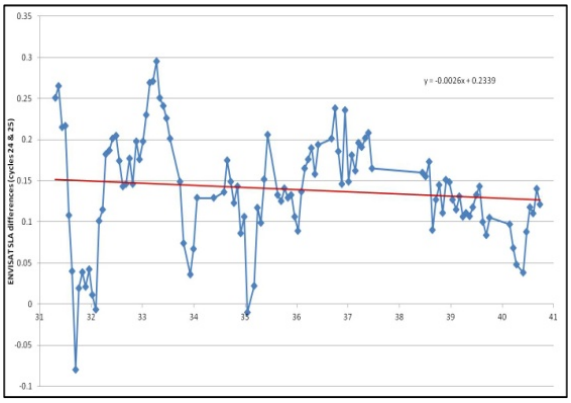

Figure 10. ENVISAT SLA differences and linear trend for pass 399 between cycles 23 and 24 (top), 23 and 25 (middle), 24 and 25 (bottom).

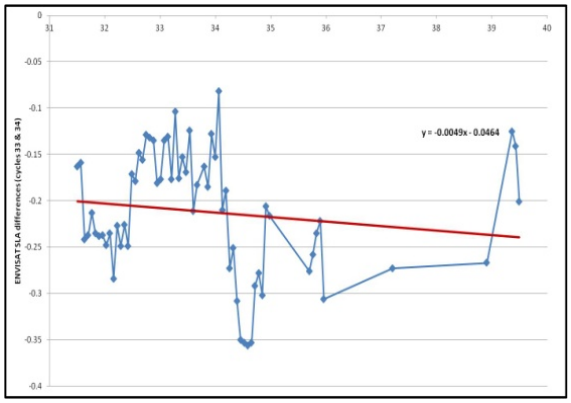

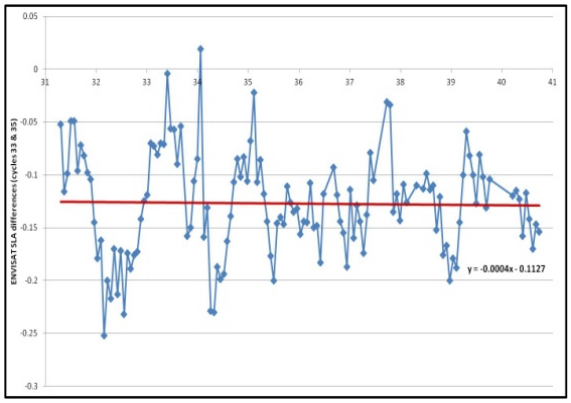

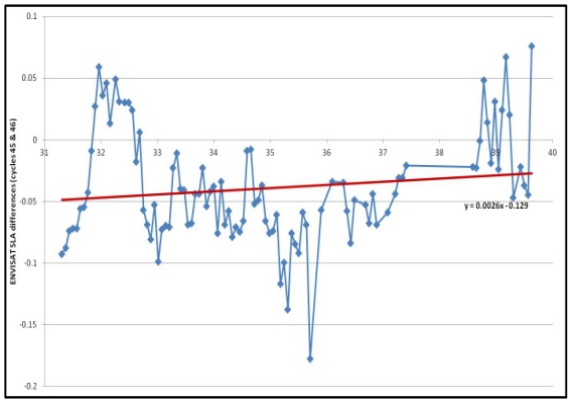

Figure 11. ENVISAT SLA differences and linear trend for pass 399 between cycles 33 and 34 (top), 33 and 35 (middle), 34 and 35 (bottom).

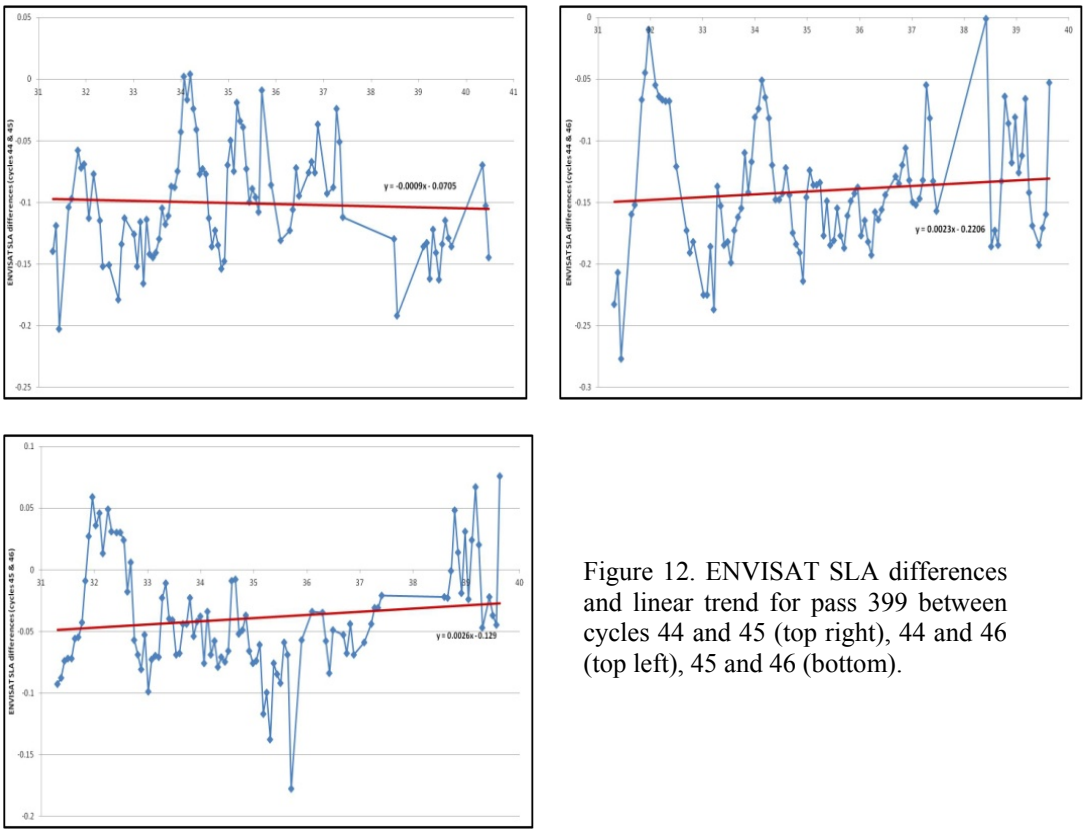

Figure 12. ENVISAT SLA differences and linear trend for pass 399 between cycles 44 and 45 (top right), 44 and 46 (top left), 45 and 46 (bottom).

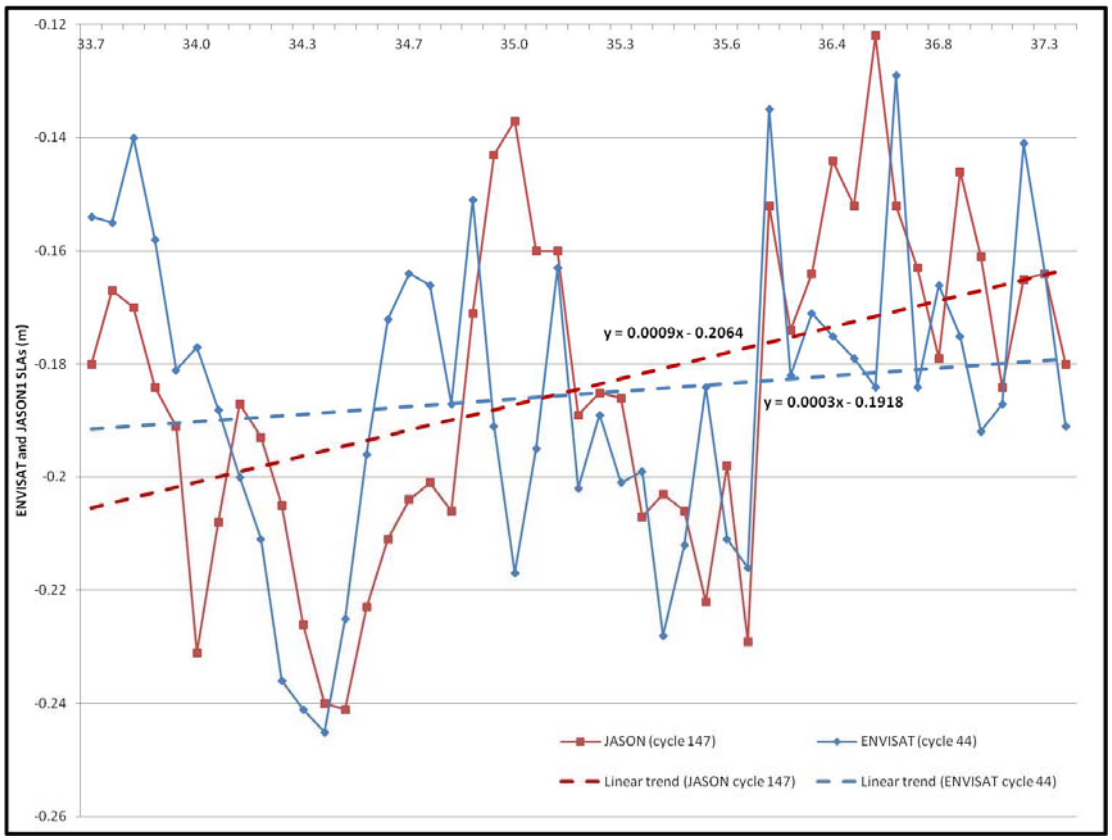

Figure 13. SLAs from ENVISAT cycle 44 along pass 399 and JASON1 cycle 147 along pass 109.

3.3. Variances and covariances as a tool for the analysis of SLA variations

As pointed out in the introductory section, the available SLAs will be used at a final stage to determine a MSS model for the wider area of the Mediterranean Sea. In LSC, and in order to construct the necessary covariance and cross-covariance matrices it is necessary to fit some analytical covariance function model to empirical values of the SLA variances, which show the statistical characteristics of the SLA field. Moreover, their variation with time can also pose an indicator for the time variations of the SLA itself and can be further correlated with large-scale oceanic effects like El Niño/La Niña. Within the scheme of the present study, the Tscherning and Rapp model was fitted to the empirical SLA covariance functions derived from the available data [30]. The variance, i.e., the covariance of the SLAs for a spherical distance of zero km, along with the correlation length can help to study the varying behaviour of the available satellite data if taken for a long enough time-period. Therefore, an analysis of the empirical covariance functions of the SLAs from ENVISAT has been carried out for the entire duration that the satellite data have been available in this study, i.e., for the time period between 2005 and 2010. Figures 15-19 below present the analytical empirical covariance functions derived for the ENVISAT SLA data along pass 444 for all consecutive months within each year between 2005 and 2010. Pass 444 was selected due to its location in the central Mediterranean Sea and the fact that it is not interrupted by islands, thus it offers a continuous record of along-track SLA (Figure 14). Given the 35-day exact repeat period of ENVISAT the collection of monthly SLA empirical covariance functions is not equal to twelve but varies between ten and eleven. In any case, for each month, only data falling in the specific time period have been used.

From the empirical covariance function for 2005 (Figure 15) it is interesting to notice the variation of the variances during the entire year. The variances range from 74 cm^2 in January, to ~30 cm^2 in February, March and April, then to 67 cm^2 in May, 52 cm^2 in June, climax to ~100 cm^2 for August, September and October and then fall again to ~70 cm^2 for November and December. This variation is in line with the thermal expansion of the sea, due to the increasing temperatures during the summer and early fall months and the lower temperatures during winter. Moreover, the seasonal cycle can be also attributed to atmospheric forcing due to the variation in atmospheric pressure in the Mediterranean. The latter can be investigated in connection with well-known climate

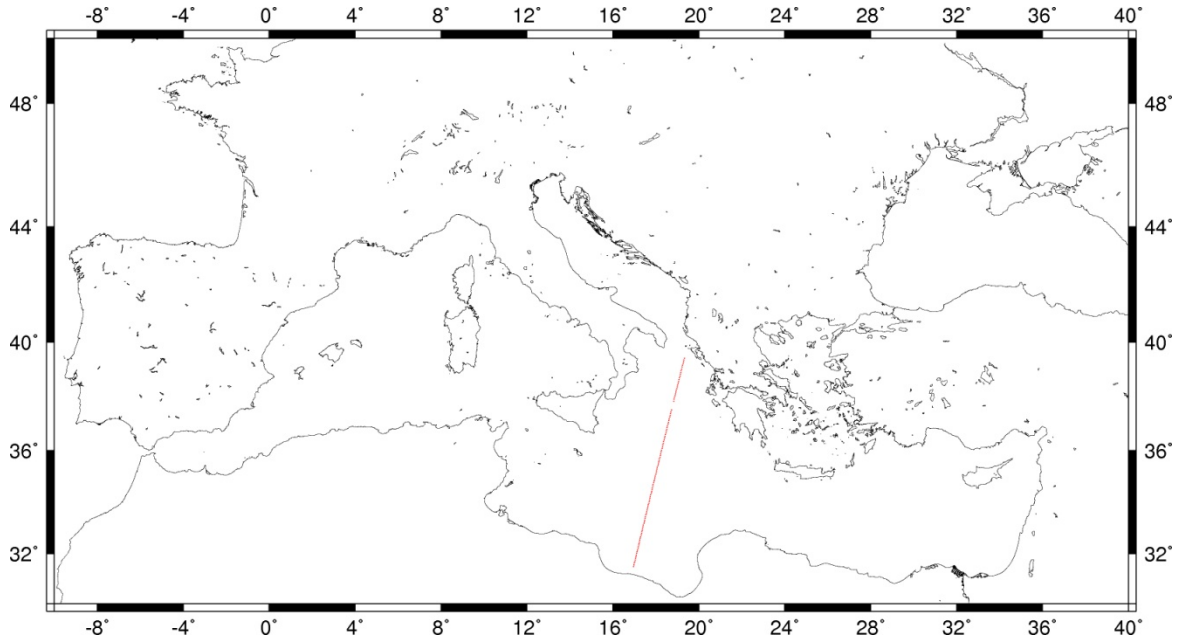

Figure 14: ENVISAT pass 444 used for the SLA empirical covariance function determination.

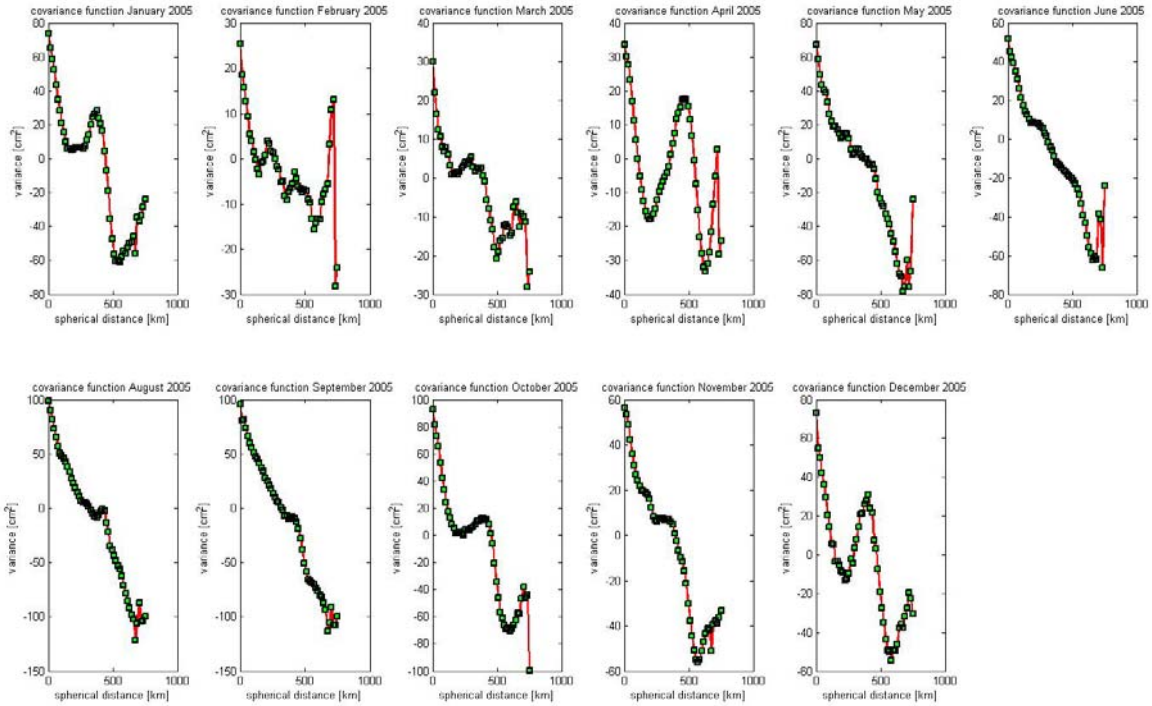

Figure 15: ENVISAT SLA empirical covariance functions in 2005.

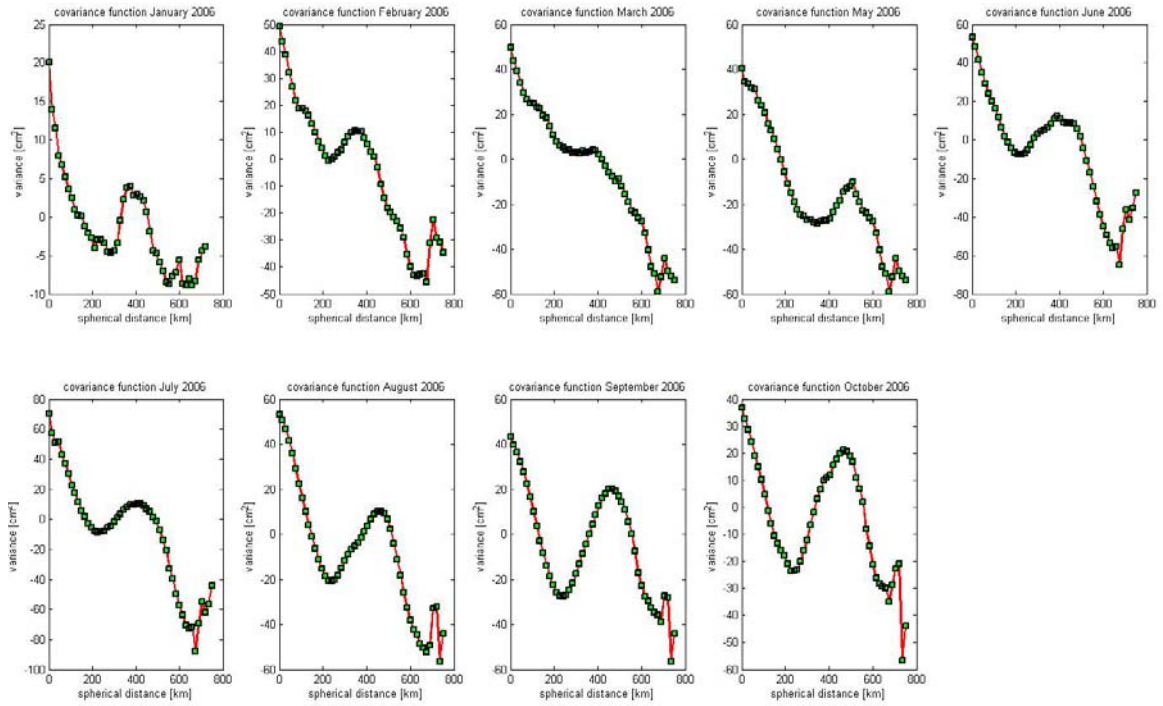

Figure 16: ENVISAT SLA empirical covariance functions in 2006.

indices like SOI, NAO and MOI. Before that step, it is interesting to see the variability of the SLA variances through time, and investigate whether come time-dependant patterns can be determined. Figure 20 depicts the variation of the SLA signal variance with time through 2005 and 2010, where also 4-month (short-dashed line) and a 6-month (long-dashed line) moving averages have been plotted to outline semi-annual and seasonal variations. From Figure 20 it is evident that there is an annual and seasonal pattern in the ENVISAT SLA variances, with the largest values occurring in

the summer months (June-July of each year) and the smallest ones in Autumn. This is more evident in the years 2008 and 2009, where large amplitude of the SLA spectra can be seen August 2008. Moreover, a significant positive trend is also evident starting from the low in May 2008 and propagating to the high amplitude in August of the same year.

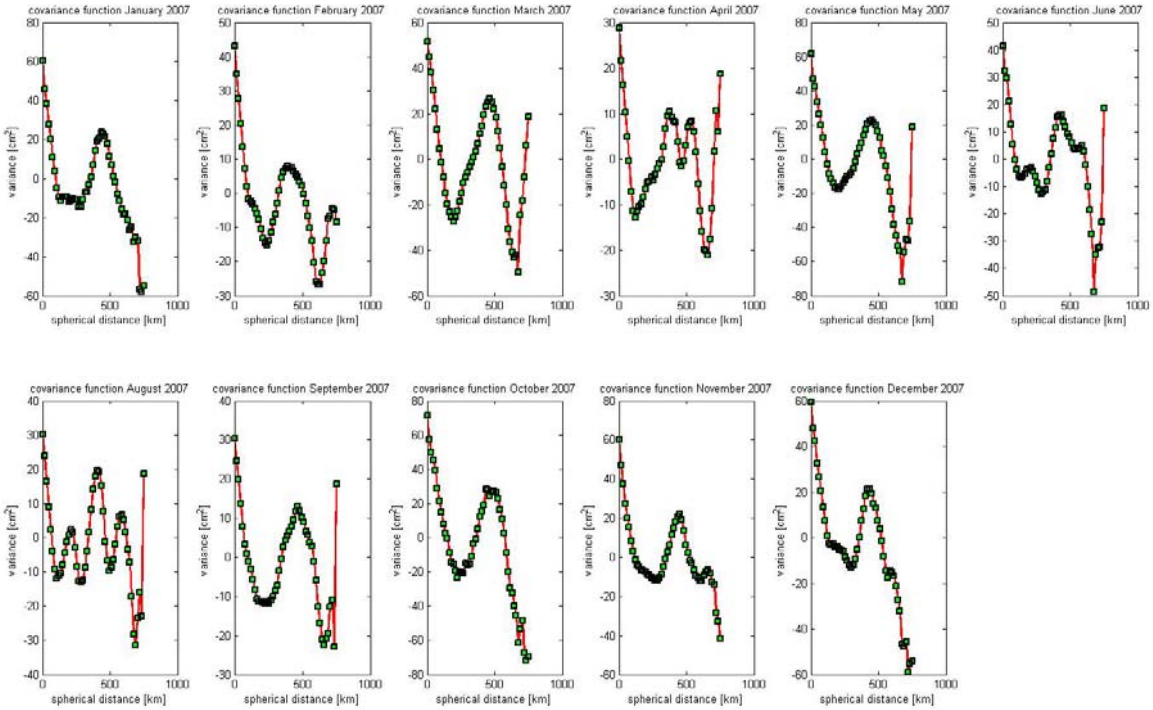

Figure 17: ENVISAT SLA empirical covariance functions in 2007.

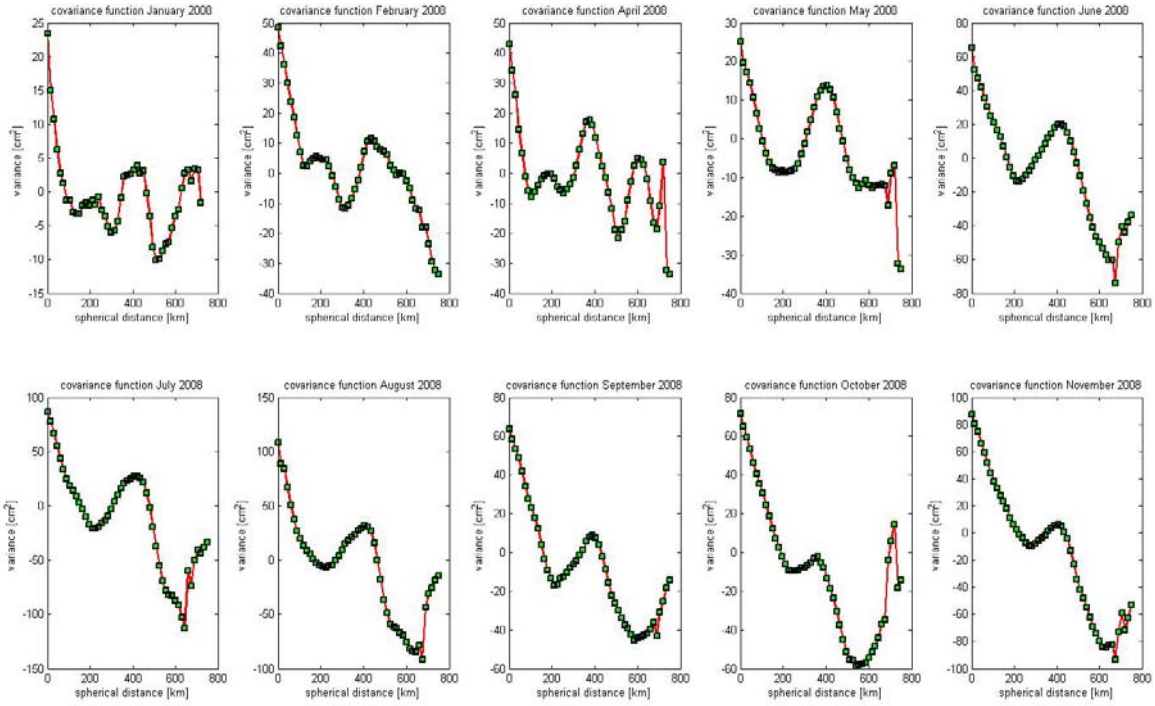

Figure 18: ENVISAT SLA empirical covariance functions in 2008.

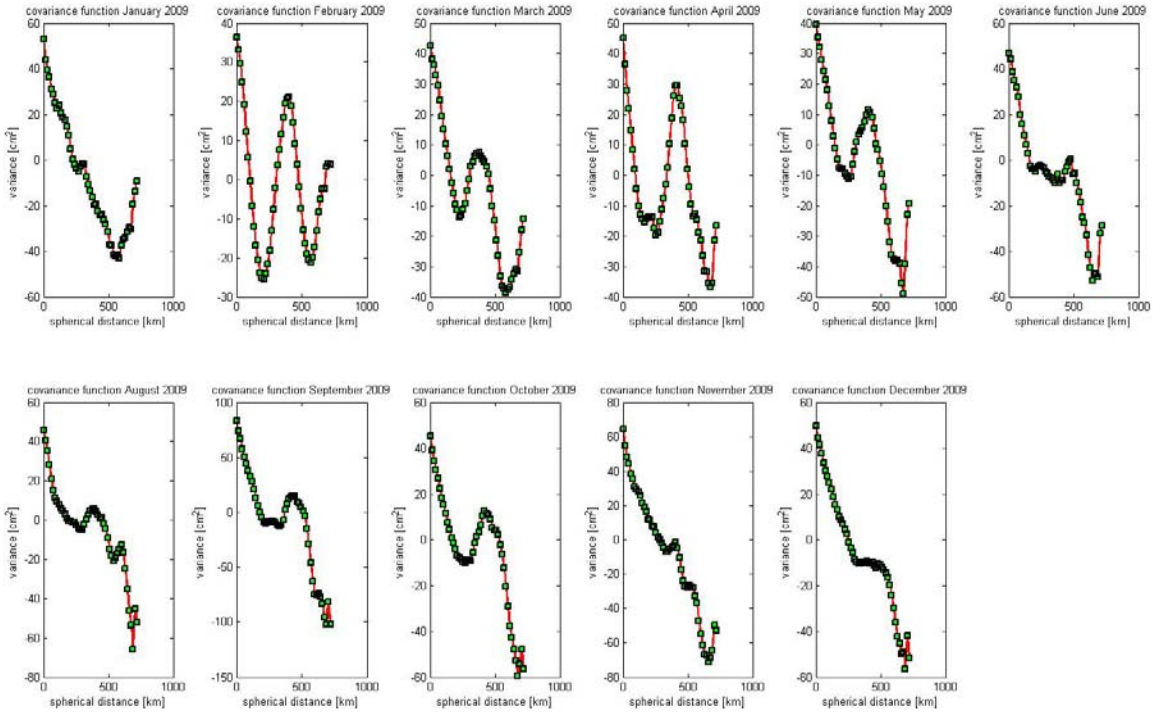

Figure 19: ENVISAT SLA empirical covariance functions in 2009.

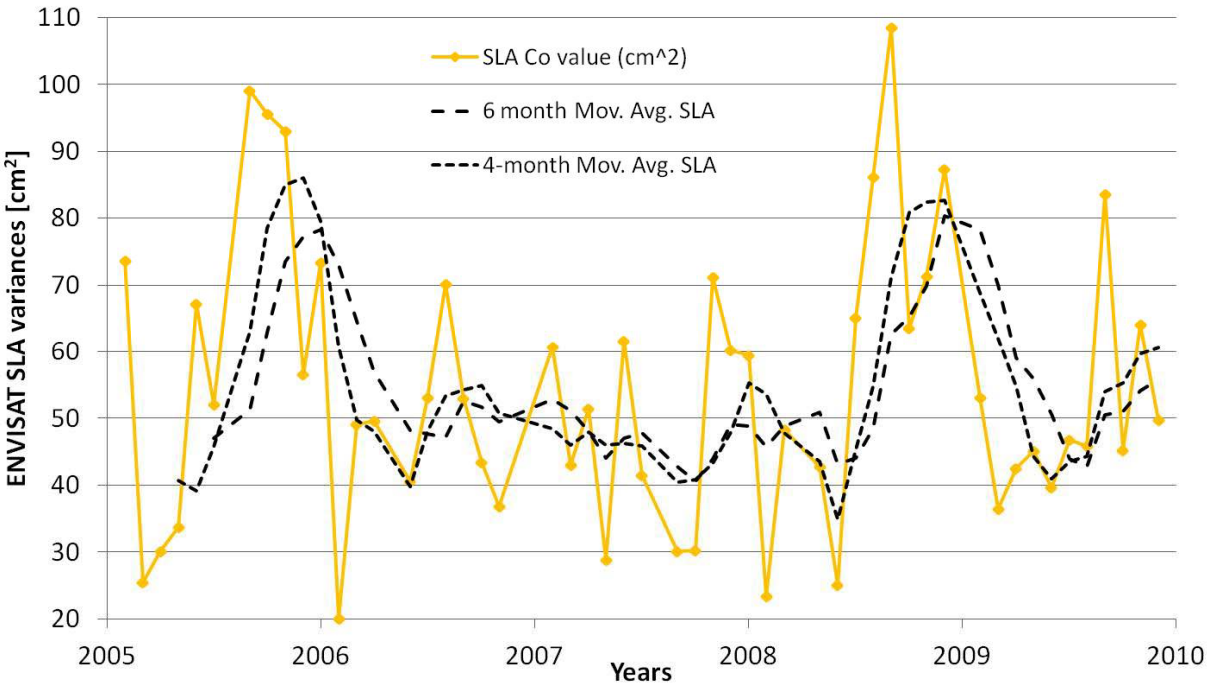

Figure 20: ENVISAT SLA variances fluctuations from 2005 to 2009.

The last step in the analysis of the SLAs is to investigate for any possible correlations with global and regional climatic phenomena that influence the ocean state as well. To this extend, three such indexes have been investigated. The first one is the well-known Southern Oscillation Index (SOI) corresponding to the ocean response to El Niño/La Niña-Southern Oscillation (ENSO) events. SOI gives an indication of the development and intensity of El Niño or La Niña events in the Pacific Ocean. It is calculated using the pressure differences between Tahiti and Darwin. Negative values of the SOI often indicate El Niño episodes, i.e., warmer waters in the eastern Tropics, while positive values of the SOI are typical of a La Niña episode, i.e., cooler waters in the eastern Tropics [36],

[37], [38]. For the present study, SOI data have been acquired from the Australian Government Bureau of Meteorology (http://www.bom.gov.au/). The next index investigated in the North Atlantic Oscillation (NAO) index, which corresponds to the fluctuations in the difference of atmospheric pressure at sea level between the Icelandic low and the Azores high. It controls winter climate variability in the North Atlantic from central North America to Europe. Positive values of the NAO result in warm and wet winters in Europe, dry winters in Mediterranean and in cold and dry winters in northern Canada and Greenland, while negative values of the NAO bring moist air into the Mediterranean and cold air to northern Europe [39, [40], 41], [42], [43]. The last index investigated is the Mediterranean Oscillation Index (MOI) which refers to the fluctuations in the difference of atmospheric pressure at sea level between Algieres and Cairo. It is an indicator of climate variability in the Mediterranean, since positive values of the MOI are related dry weather throughout the Mediterranean, except from the south-eastern part. On the contrary negative values of MOI are related to cyclogenesis in west Mediterranean and abnormally wet weather, except from the south-eastern part [44], [45], [46], [47]. For the present study, NAO and MOI data have been acquired from the Climate Research Unit of the University of East Anglia (http://www.cru.uea.ac.uk/)

To analyse any possible correlations, the ENVISAT SLA variances for pass 444 (Figure 14) have been compared for the period between 2005 and 2010 with the SIO, NAO and MOI indexes. Figure 21 below depicts the ENVISAT SLA variances for the period under study, along with the SOI indexes for the same time span. From that Figure it can be concluded that some correlation between ENSO events and SLA variations in the Meditteranean can be seen, even though with a phase offset of ~4-8 months. The large negative values at the beginning of 2005 (February) are related to the highs in Mediterranean SLAs which appear in July of 2005. The El Niño appearance in March 2006 has a more rapid signature in the Mediterranean SLA data since it results in significant increase in the SLA in June-July 2006, i.e., a time period of 5 months. The same behaviour is evidences for the La Niña events too, as can be seen for the strong occurrences in late 2007-early 2008 and in late 2008-early 2009. These results in significant depressions in the SLA variances which reach their smallest values in April 2008 and February 2009, i.e., with a time lag of ~4 months.

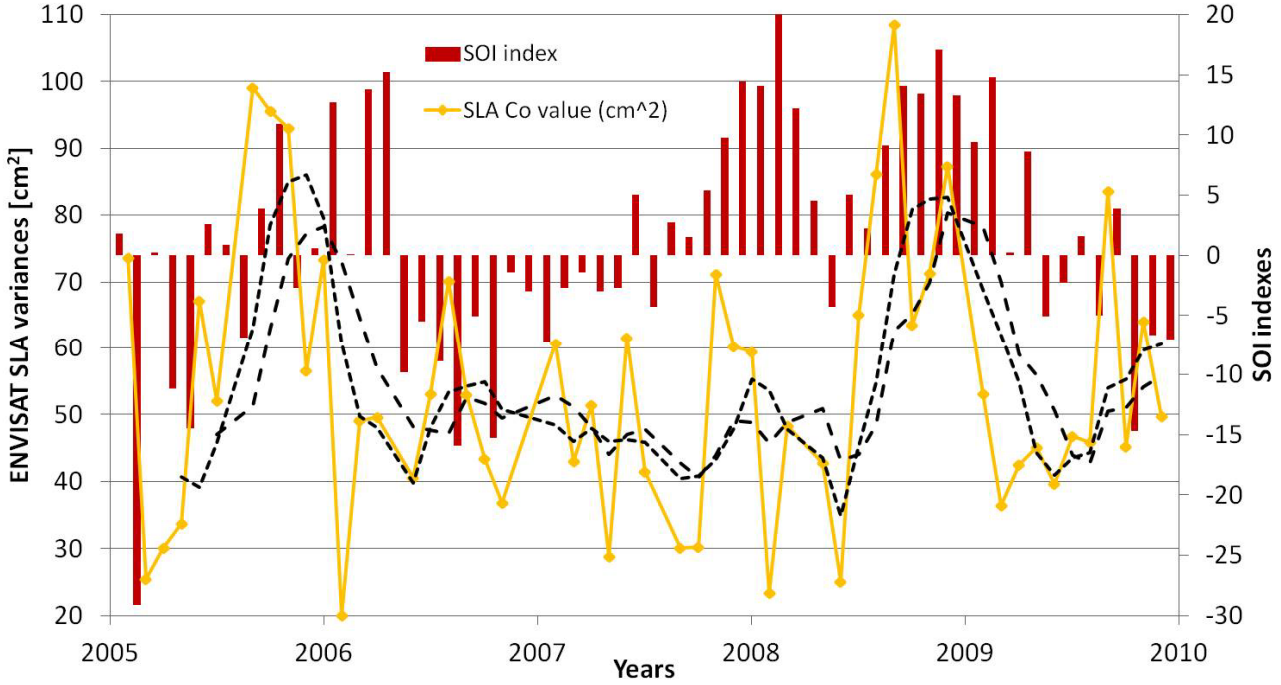

Figure 21: ENVISAT SLA variances fluctuations from 2005 to 2009 and correlation with SOI.

Given that El Niño and La Niña may not be representative for the Mediterranean Sea due to their distance and the characteristics of the latter as a closed sea area, the NAO index should be more appropriate to indicate any correlation between atmospheric forcing and SLA variations. Figure 22 depicts the ENVISAT SLA variances for the period under study, along with the NAO indexes for the same time span. It is now evident that a stronger correlation can be seen, since the positive NAO values are related to more immediate depressions in the Mediterranean sea level, while negative ones to increased sea levels. Noticing are the large positive NAO values at the beginning of 2007 which are immediately depicted as depressions in the Mediterranean SLA with a time lag of less than one month. The same behaviour is found for all winter months, i.e., a good correlation, while for summer months the response of the Mediterranean sea level to variations in NAO is not so well depicted. This is in-line with the findings from related work (see, e.g., [45]), which signals that atmospheric forcing is not the contributing factor to the steric sea level variations in the Mediterranean during the summer period.

To assess that, the MOI has been investigated as well, since it should be the most proper measure of atmospheric forcing contribution to sea level variations in the Mediterranean. Figure 23 depicts the ENVISAT SLA variances for the period under study, along with the MOI indexes for the same time span. For the visualization and comparison to be easier, given that the MOI data were available as daily values, a 30-day mean has been plotted as well. From Figure 23 it becomes clear that positive phases in MOI are related to depressions in the SLA due to dryer conditions, as can be seen in July 2007 and February 2009. The same behaviour can be seen for the negative MOI values which result in increased sea level as for example in early 2005 and September 2007. Some very large positive trends in the SLA though are not directly correlated with MOI, as for instance in August 2008, where a positive MOI is related to larger SLAs. On the contrary, at the same time period the NAO index presents a large negative value, signaling the interrelation of the Atlantic circulation and the variability in the Mediterranean. This anti-correlation between NAO and MOI for the summer of 2008 can be seen from Figure 24 as well, where the two indexes are plotted alongside. Even though in most cases NAO and MOI are well correlated and follow each other, especially during Winter and Autumn, their disagreement in Spring and Summer signals that atmospheric conditions in the North Atlantic are not the dominant contributing factor for the Mediterranean Sea.

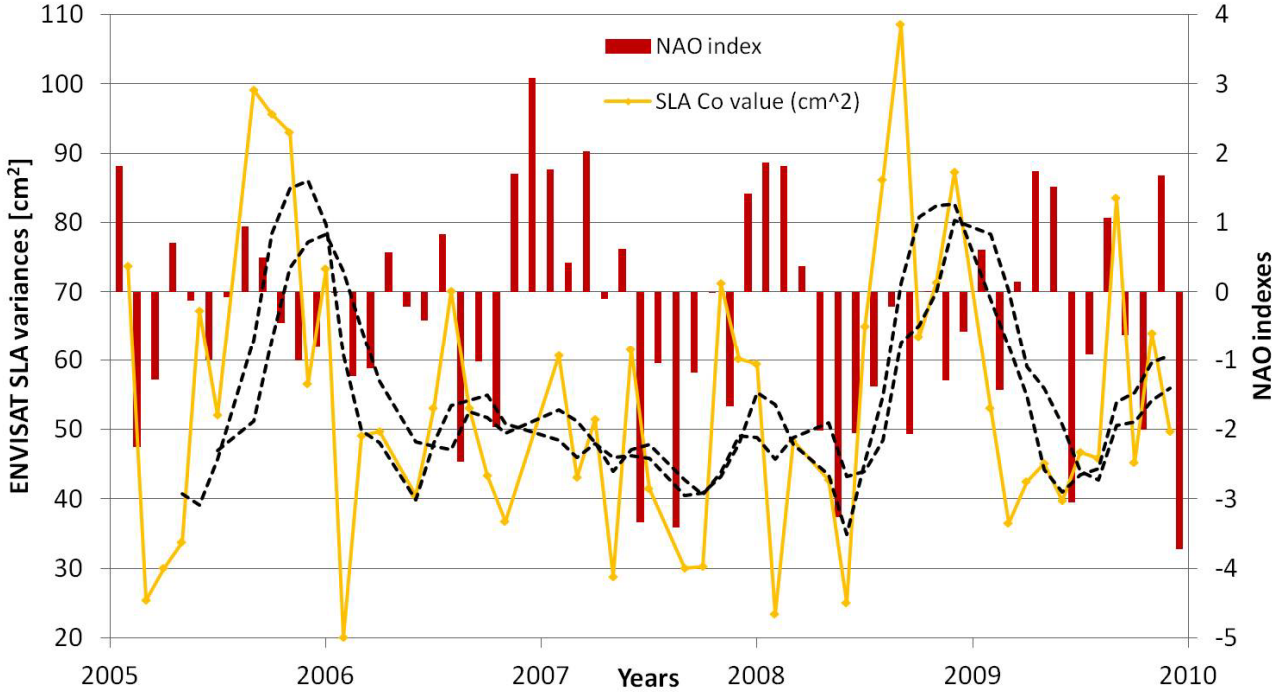

Figure 22: ENVISAT SLA variances fluctuations from 2005 to 2009 and correlation with NAO.

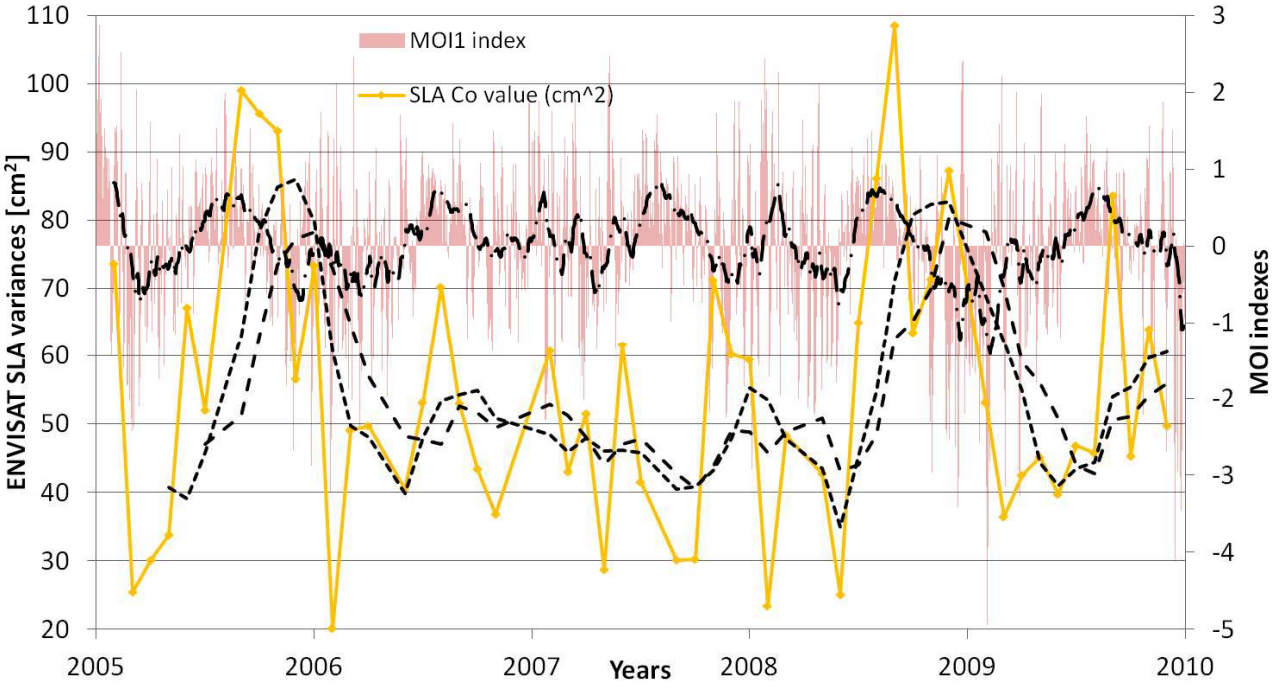

Figure 23: ENVISAT SLA variances fluctuations from 2005 to 2009 and correlation with MOI.

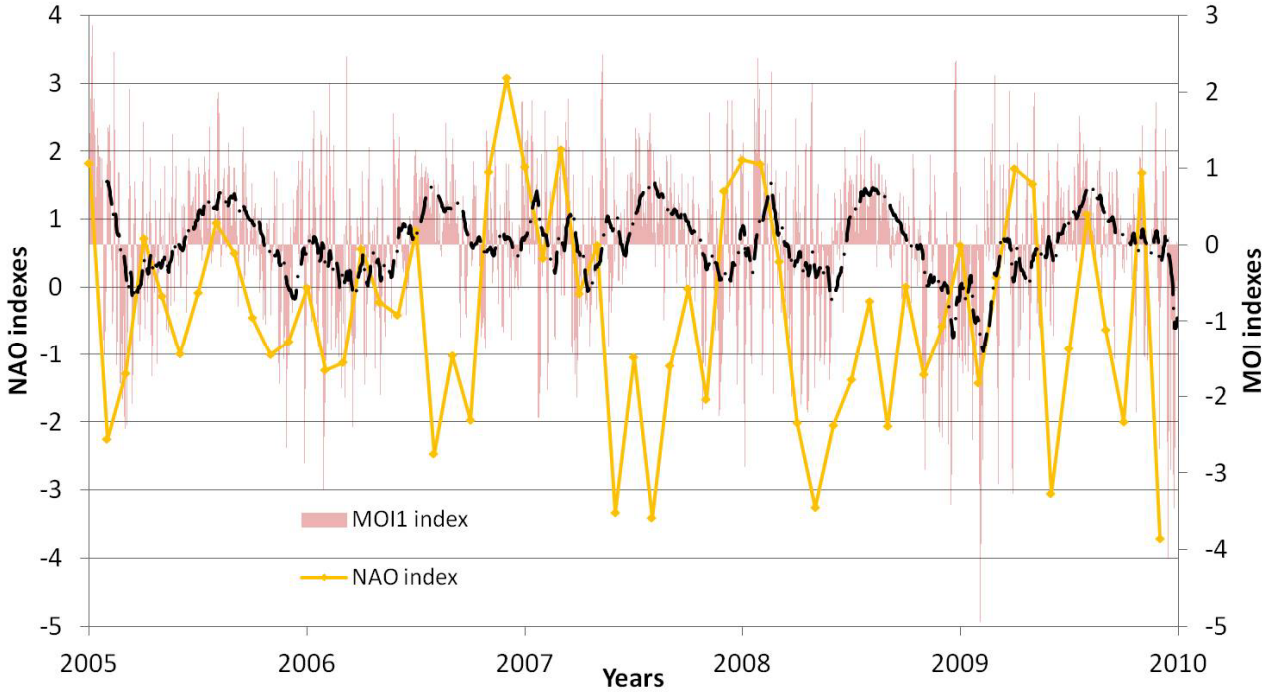

Figure 24: NAO and MOI indexes for the period between 2005 and 2010.

4. Mean sea surface model development

Following the analysis of the JASON1 and ENVISAT SLAs, the available data have been used to determine a Mean Sea Surface (MSS) model for the Mediterranean Sea. Given that the SLA records are referenced to the EGM2008 model [34] the contribution of that global geopotential model, full to degree and order 2159, has been evaluated to the final MSS grid nodes. The final model was

selected to have a 5′×5′ spatial resolution, therefore EGM2008 geoid heights have been estimated to that grid in the zero-tide system in order to conform with the tide conventions adopted for the altimetric data processing. Table 6 presents the statistics of the EGM08 contribution to geoid heights for the area under study, which covers the entire Mediterranean Sea.

Table 6. Statistics of a) the EGM2008 contribution to geoid heights for the area under study, b) the final MSS model and c) its differences with DTU2010. Unit: [m].

	min	max	mean	std
EGM2008	-0.906	59.401	37.780	±12.413
MSS (5′×5′)	0.847	59.527	37.818	±12.374
MSS-DTU2012	-2.527	0.743	0.002	±0.080

In order to determine the MSS model, the available SLAs from JASON1 and ENVISAT after the 3σ test have been used (Table 3). These SLAs are utilised in the frame of LSC in order to estimate the 5′×5′ MSS model, so first the empirical covariance function has been estimated in order to derive the necessary parameters, which were then used to estimate the SLA on the required reference grid. Figure 25 below presents the empirical covariance function of the combined, multi-satellite SLA dataset, from which a variance of 0.0156 m^2 and a correlation length of ~280 km were found. The evaluation of the empirical covariance function and the subsequent fit of the Tscherning and Rapp model [30] to these empirical values have been evaluated with the Gravsoft suite of programs [48]. Using the parameters determined from the fit of the analytical model (i.e., depth to *Bjerhamar* sphere, fitted variance and scale factor), together with the error degree variances of the EGM2008 model, the final LSC-based prediction on the 5′×5′ nodes has been carried out. Finally, the MSS model has been determined by restoring the contribution of EGM2008. Table 6, middle row, summarizes the statistics of the estimation MSS model for the Mediterranean Sea, while the model itself is depicted in Figure 26.

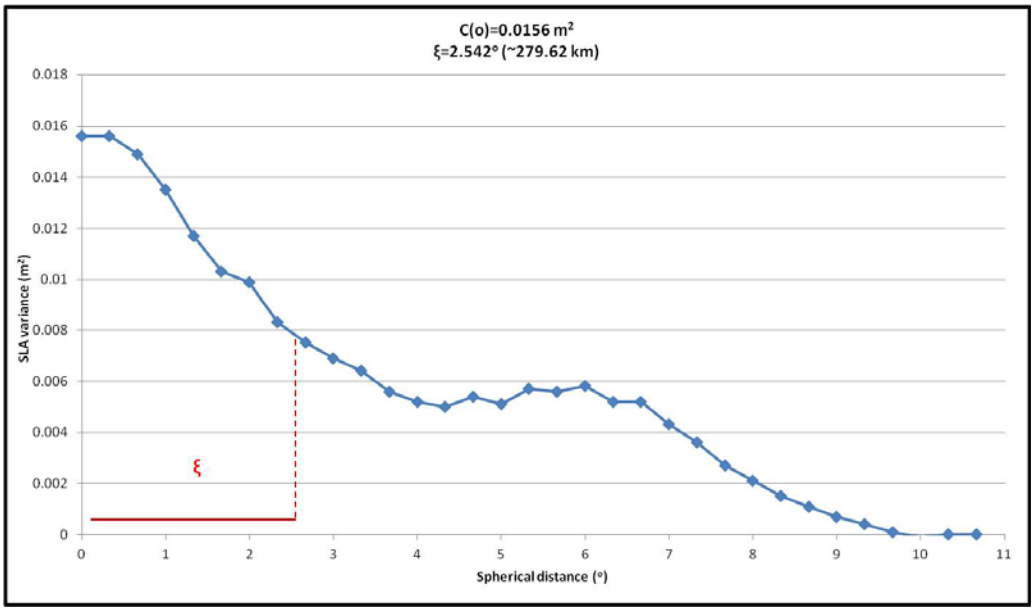

Figure 25: Combined JASON1 and ENVISAT SLA empirical covariance function.

In order to evaluate the estimated MSS model, a comparison with the latest Mean Sea Model from the Danish Space Agency, namely DNSC2010 [10], [11], [49] has been carried out. The statistics of the differences are presented in Table 6 (last row) which Figure 26 (bottom) depicts

them for the entire area under study. As it can be seen from both the Table and the Figure, the statistics are quite satisfactory, since the std of the differences is at the ±8 cm level only, with the mean value almost at zero. In purely marine areas, the developed MSS model agrees vary well with DNSC2010 (all differences between -5 and 5 cm), while the largest deviations are found only along coastal areas, where special retracked altimetric data have been used in DNSC2010. Such data and processing methodologies have not been considered in the developed MSS model, therefore such large differences in coastal areas are expected. If a mask of 20 km is used around the coastline, in order to consider purely marine areas, then the std of the differences reduces to 4 cm only and the range is between -50 and 50 cm. This is good evidence that the so-derived MSS model is comparable with global ones, which are based on far more data sources (practically all available satellite altimetry data are used, from GEOSAT and ERS1 to JASON2 and ENVISAT) and sophisticated data treatment.

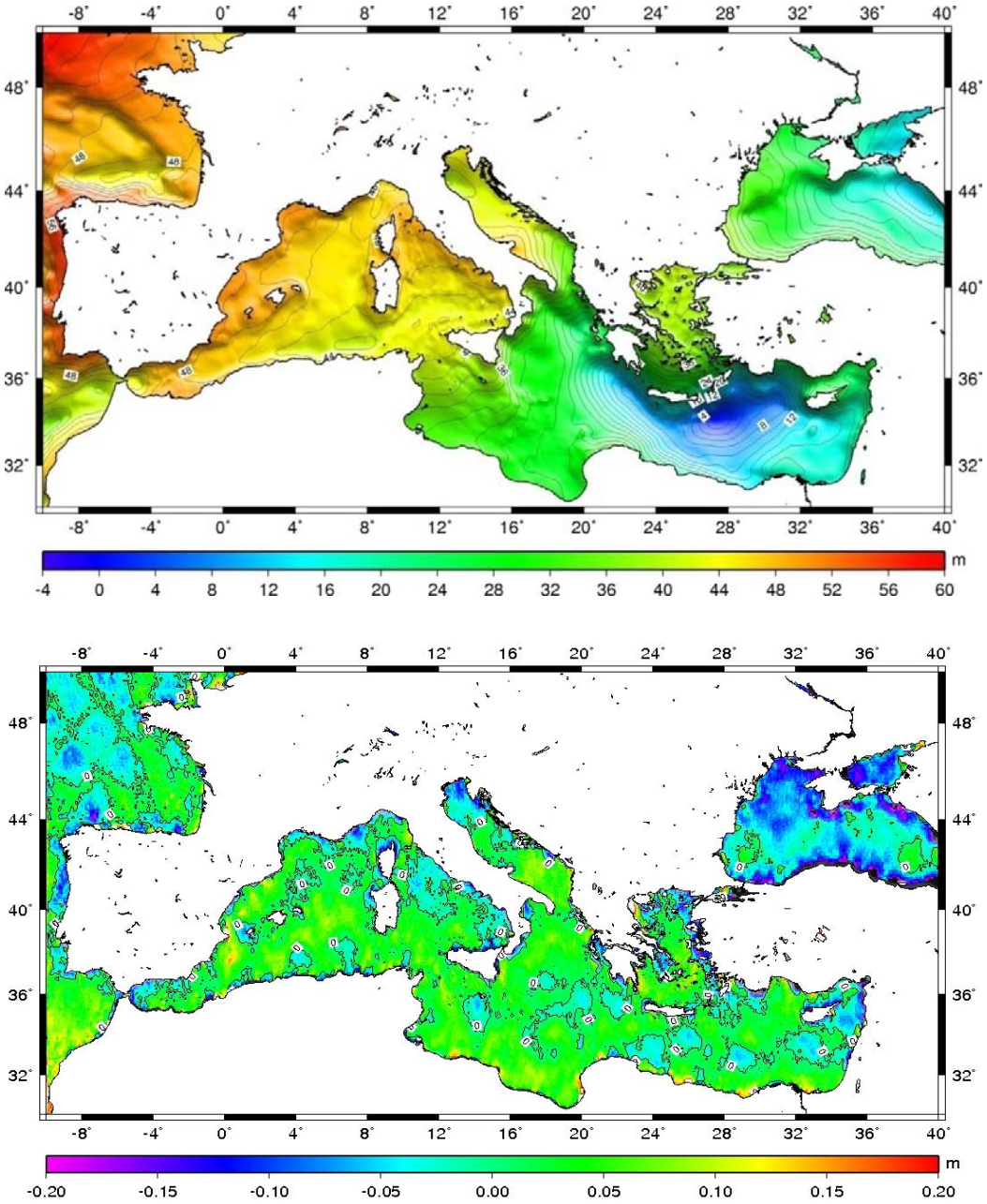

Figure 26: The final combined JASON1 and ENVISAT MSS model from LSC (top) and its differences with DTU2010 (bottom).

5. Conclusions

An analytical outline of the use of satellite altimetry data from the exact repeat missions of JASON1 and ENVISAT to monitor SLA variations has been presented. The study referred to the detection of trends in the sea level, either rise or fall, for short time periods between 10 and days and 3 months, based on geophysically and IB corrected altimetric records. The data analysed referred to along-track records for two tracks that span the entire Mediterranean Sea in the north-south direction. From that analysis, trends between -2 cm/10-days and 3 cm/10-days have been determined, showing that the sea level has significant variations, which are not wind and/or pressure driven, even at such small time intervals.

When longer time intervals of the order of 35-days to 3-months are investigated, these trends are significantly reduced, something expected since short-time variations are smoothed out. In that case the trends determined from ENVISAT data are of the order of ~3-6 mm per 35-days to 3-motnhs and are in agreement with the 20-year long global trends identified from the analysis of all available altimetric records.

From the analysis of the empirical covariance functions of ENVISAT SLA, it was noticed that there is a significant annual variation which is evident for the entire period under study. The variances for 2005 ranged from 74 cm^2 in January, to ~30 cm^2 in February, March and April, then to 67 cm^2 in May, 52 cm^2 in June, climax to ~100 cm^2 for August, September and October and then fall again to ~70 cm^2 for November and December. This variation is in line with the thermal expansion of the sea, due to the increasing temperatures during the summer and early fall months and the lower temperatures during winter. Moreover, the seasonal cycle can be also attributed to atmospheric forcing due to the variation in atmospheric pressure in the Mediterranean.

From the comparison of the SLA variations in the Mediterranean with climatic indexes like SIO, NAO and MOI it was found that El Niño and La Niña has a response to the Mediterranean as well but with a time lag ranging from 4-8 months, depending on the strength of the ENSO events. In the analysis with NAO it was found that for all winter months a good correlation exists, while for summer months the response of the Mediterranean sea level to variations in NAO is not so well depicted. On the other hand, the response of the Mediterranean Sea to atmospheric forcing within its vicinity is more predominant, since from the comparisons of the SLAs with MOI it became clear that positive phases in MOI are related to depressions in the SLA due to dryer conditions, as can be seen in July 2007 and February 2009. It can be concluded that even though in most cases NAO and MOI are well correlated and follow each other, especially during Winter and Autumn, their disagreement in Spring and Summer signals that atmospheric conditions in the North Atlantic are not the dominant contributing factor for the Mediterranean Sea.

Finally, the available along-track JASON1 and ENVISAT SLAs, have then been used to determine a Mediterranean-wide MSS model. The estimation was based on LSC for the prediction of the SLA on the final 5′×5′ nodes, while the resulting model presents a very good agreement with the latest global MSS model, namely DTU2010. The standard deviation of the developed MSS with DTU2010 is at the ±8 cm level, while when purely marine areas are considered, after the application of a 20 km wide coastline mask, it reduced to ±4 cm only.

Acknowledgements

We extensively used the Generic Mapping Tools [50] in displaying our results.

References

[1] Mediterranean Action Plan – MAP, 2012. Available from: http://www.unepmap.org/. Accessed April 2012.

[2] American Association for the Advancement of Science - AAAs, 2011. Coasts and the population bomb. Available from: http://www.aaas.org. Accessed December 2011.

[3] CCSP (U.S. Climate Change Science Program), 2009. Coastal Sensitivity to Sea-Level Rise: A Focus on the Mid-Atlantic Region. Available from: http://www.climatescience.gov/Library/sap/sap4-1/final-report/default.htm. Accessed December 2011.

[4] GCRP (U.S. Global Change Research Program, 2009. Global Climate Change Impacts in the United States. Available from: http://www.globalchange.gov/usimpacts. Accessed December 2011.

[5] Burkett, V. R., Zilkoski, D. B. and Hart, D. A. 2005. Sea-level rise and subsidence: Implications for flooding in New Orleans, Louisiana. In: Subsidence observations based on traditional geodetic techniques, and numerical models. U.S. Geological Survey, National Wetlands Research Center. Available from: http://www.nwrc.usgs.gov/hurrica ne/Sea-Level-Rise.pdf [Accessed December 2011].

[6] Douglas, B. C., 1997. Global Sea Rise: A Redetermination. *Surveys in Geophysics*, 18: 279-292.

[7] EPA - USA Environmental Protection Agency, 2011. Sea Level. Available from: http://cfpub.epa.gov/eroe/index.cfm?fuseaction=detail.viewInd&lv=list.listbyalpha&r=216636&subtop=315. Acessed December 2011.

[8] AVISO, 2011. Available from: http://www.aviso.oceanobs.com/en/altimetry/principle/basic-principle/. Accessed October 2011.

[9] Chelton, D. B., Ries, J. C., Haines, B. J., Fu, L. L. and Callahan, P., 2001. Satellite Altimetry. In: Fu LL, Cazenave A (eds) Satellite Altimetry and Earth Sciences A Handbook of Techniques and Applications. *International Geophysics Series* 69: 1-132, Academic Press, San Diego, California.

[10] Andersen, O. B., 2010. The DTU10 Gravity field and Mean sea surface. Second international symposium of the gravity field of the Earth (IGFS2010), Fairbanks, Alaska.

[11] Andersen OB & P Knudsen, 1998. Global marine gravity field from the ERS1 and Geosat geodetic mission. *J Geophys Res*, 103: 8129-8137.

[12] Cazenave, A., Schaeffer, R., Berge, M., Brosier, C., Dominh, K. and Genero, M. C., 1996. High-resolution mean sea surface computed with altimeter data of ERS1 (geodetic mission) and TOPEX/POSEION. *Geophys J Int*, 125: 696-704.

[13] Yi, Y., 1995. *Determination of gridded mean sea surface from altimeter data of TOPEX, ERS-1 and GEOSAT*. Rep of the Dept of Geodetic Sci and Surv No 434 The Ohio State Univ, Columbus, Ohio.

[14] Arabelos, D. and Tziavos, I. N., 1996. Combination of ERS1 and TOPEX altimetry for precise geoid and gravity recovery in the Mediterranean Sea. *Geophys J Int*, 125: 285-302.

[15] Natsiopoulos, D. A., 2010. Determination of mean sea surface and sea level anomaly models in different regional and temporal scales by altimetric data. Diploma Theses, Department of Geodesy and Surveying, Aristotle University of Thessaloniki, Greece, June 2010.

[16] Tziavos, I. N., Forsberg, R. and Sideris, M. G., 1998. Marine Gravity Field modelling Using Shipborne and Geodetic Missions Altimetry Data. *Geomatics Research Australasia*, 69:1-18.

[17] Tziavos, I. N., Vergos, G. S. and Kotzev, V., Pashova, L., 2005. Mean sea level and sea surface topography studies in the Black Sea and the Aegean. *International Association of Geodesy Symposia*, Vol. 129, Jekeli C, Bastos L, Fernandes J (eds.), Gravity Geoid and Space Missions 2004, Springer – Verlag Berlin Heidelberg: 254-259.

[18] Vergos, G. S., 2002. *Sea Surface Topography, Bathymetry and Marine Gravity Field Modelling*. UCGE Rep Nr 20157, Calgary AB, Canada.

[19] Vergos, G. S., Tziavos, I. N. and Andritsanos, V. D., 2005a. *On the Determination of Marine Geoid Models by Least-Squares Collocation and Spectral Methods Using Heterogeneous Data*. In: Sansó F (ed.) A Window on the Future of Geodesy, Inter Assoc of Geod Symposia, vol. 128, Springer – Verlag Berlin Heidelberg, 332-337.

[20] Vergos, G. S., Tziavos, I. N. and Andritsanos, V. D. 2005b. *Gravity Data Base Generation and Geoid Model Estimation Using Heterogeneous Data*. In: Jekeli C, Bastos L, Fernandes J (eds.) Gravity Geoid and Space Missions 2004, Inter Assoc of Geod Symposia, vol. 129, Springer – Verlag Berlin Heidelberg, 155-160.

[21] Vergos, G. S., Grigoriadis, V. N., Tziavos, I. N. and Sideris, M. G., 2007. *Combination of multi-satellite altimetry data with CHAMP and GRACE EGMs for geoid and sea surface topography determination*. In: Tregoning P, Rizos C (eds) Dynamic Planet 2005 - Monitoring and Understanding a Dynamic Planet with Geodetic and Oceanographic Tools, International Association of Geodesy Symposia, vol.130 Springer – Verlag Berlin Heidelberg, pp. 244-250.

[22] Cazenave, A. and Nerem, R. S., 2004. *Present-day sea-level change: Observations and causes*. Reviews in Geophysics, 42 (RG3001), doi:10.1029/2003RG000139.

[23] Church, J. A., White, N. J., Konikow, L. F., Domingues, C. M., Cogley, J. G., Rignot, E., Gregory, J. M. van den Broeke, M. R., Monaghan, A. J. J. and Velicogna, I., 2011. Revisiting the Earth's sea-level and energy budgets from 1961 to 2008. *Geophys Res Lett*, (38) L18601. doi:10.1029/2011GL048794.

[24] Nerem, R. S., Leuliette, E. and Cazenave, A., 2006. Present-day sea-level change: A review. *Comptes Rendus Geosciences*, 338; 1077-1083.

[25] Nerem, R. S. and Mitchum, G. T., 2001. *Sea Level Change*. In: Fu L.-L. and Cazenave A (eds) Satellite Altimetry and Earth Sciences. Int Geophys Series Vol 69, Academic Press, San Diego California, 329-350.

[26] Tapley, B. D. and Kim M-G, 2001. *Applications to Geodesy*. In: Fu L.-L. and Cazenave A (eds) Satellite Altimetry and Earth Sciences. Int Geophys Series Vol 69, Academic Press, San Diego California, 371-406.

[27] Barzaghi, R., Maggi, A., Tselfes, N., Tsoulis, D., Tziavos, and I. N. and Vergos, G. S. 2009a. *Combination of Gravimetry, Altimetry and GOCE Data for Geoid Determination in the Mediterranean: Evaluation and Simulation*. In: Sideris MG (ed) Observing our Changing Earth, International Association of Geodesy Symposia Vol. 133, Springer Berlin Heidelberg New York, pp. 195-202.

[28] Barzaghi, R., Tselfes, N., Tziavos, I. N. and Vergos, G. S. 2009b. Geoid and High Resolution Sea Surface Topography Modelling in the Mediterranean from Gravimetry, Altimetry and GOCE Data: Evaluation by Simulation. *Journal of Geodesy*, 83(8):751-772. doi: 10.1007/s00190-008-0292-z.

[29] Sansò, F., Venuti, G., Tziavos, I. N., Vergos, G. S. and Grigoriadis, V. N. 2008. Geoid and Sea Surface Topography from satellite and ground data in the Mediterranean region - A review and new proposals. *Bulletin of Geodesy and Geomatics*, 67(3): 155-201.

[30] Tscherning, C. C. and Rapp, R. H., 1974. Closed Covariance Expressions for Gravity Anomalies, Geoid Undulations, and Deflections of the Vertical Implied by Anomaly Degree-Variance Models. Rep of the Dept of Geodetic Sci and Surv No 208 The Ohio State Univ, Columbus, Ohio.

[31] RADS-DEOS, 2011. Available from: http://rads.tudelft.nl (Radar Altimeter Database System). Accessed January 2011.

[32] AVISO User Handbook, 1998. Corrected Sea Surface Heights (CORSSHs) AVI-NT-011-311-CN Edition 31.

[33] Fernandes JM, S Barbosa & C Lázaro, 2006. Impact of Altimeter Data Processing on Sea Level Studies. Sensors, 6: 131-163.

[34] Pavlis, N. K., Holmes, S. A., Kenyon, S. C. and Factor, J. K., 2008. An Earth Gravitational Model to Degree 2160: EGM2008, *presented at the 2008 General Assembly of the European Geosciences Union*, Vienna, Austria, April 13-18, 2008.

[35] Naeije, M., Scharroo, R., Doornbos, E. and Schrama, E., 2008. *GLobal Altimetry Sea-level Service: GLASS*. Final Report. NIVR/DEOS publ., NUSP-2 report GO 52320 DEO, 107pp, December 2008.

[36] Allan, R. J., Nicholls, N., Jones, P. D. and Butterworth, I. J., 1991. A further extension of the Tahiti-Darwin SOI, early SOI results and Darwin pressure. *J. Climate*, 4: 743-749.

[37] Können, G.P., Jones, P. D., Kaltofen, M. H. and Allan, R. J., 1998. Pre-1866 extensions of the Southern Oscillation Index using early Indonesian and Tahitian meteorological readings. *J. Climate*, 11: 2325-2339.

[38] Ropelewski, C. and Jones, P. D., 1987. An extension of the Tahiti-Darwin Southern Oscillation Index. *Monthly Weather Review*, 115: 2161-2165.

[39] Tsimplis, M. N. and Josey, S. A., 2001. Forcing of the Mediterranean Sea by atmospheric oscillations over the North Atlantic. *Geophysical Research Letters*, 28(5): 803-806.

[40] Osborn, T. J., 2006. Recent variations in the winter North Atlantic Oscillation. *Weather*, 61: 353-355.

[41] Osborn, T. J., 2011. Winter 2009/2010 temperatures and a record-breaking North Atlantic Oscillation index. *Weather*, 66: 19-21.

[42] Wakelin, S. L., Woodworth, P. L., Flather, R. A. and Williams, J. A., 2003. Sea-level dependence on the NAO over the NW European Continental Shelf. *Geophysical Research Letters*, 30(7), 1403, doi:10.1029/2003GL017041.

[43] Woolf, D. K., Shaw, A. G. P. and Tsimplis, M. N., 2003. The influence of the North Atlantic Oscillation on Sea Level Variability in the North Atlantic Region. *The Global Atmosphere and Ocean System*, 9(4): 145-167.

[44] Palutikof, J. P., 2003. *Analysis of Mediterranean climate data: measured and modelled*. In: Bolle, H.J. (ed): Mediterranean climate: Variability and trends. Springer-Verlag, Berlin.

[45] Tsimplis, M. N. and Shaw, A. G. P., 2008. The forcing of mean sea level variability around Europe. *Global and Planetary Change*, 63(2–3): 196-202, doi 10.1016/j.gloplacha.2007.08.018.

[46] Supic, M., Grbec, B., Vilibic, I. and Ivancic, I., 2004. Long-term changes in hydrodynamical conditions in Northern Adriatic and its relationship to hydrological and atmospheric processes, *Ann. Geophys.*, 22 (3): (2004), pp. 733–745

[47] Sušelj, K. and Bergant, K., 2006. Mediterranean Oscillation Index Geophys. *Res. Abstr.*, 8 (2006), p. 02145 European Geosciences Union.

[48] Forsberg, R., and Tscherning, C. C., 2008. *An overview manual for the GRAVSOFT Geodetic Gravity Field Modelling Programs*. 2nd ed.

[49] Andersen, O. B. and Knudsen, P., 2009. The DNSC08 mean sea surface and mean dynamic topography. *J Geophys Res*, 114(C11) doi:10.1029/2008JC005179.

[50] Wessel, P. and Smith, W. H. S., 1998. New improved version of Generic Mapping Tools released. *EOS Trans. Amer. Geophys. U.*, 79(47): 579.